Tailoring Casimir interactions with nanostructures

Diego A. R. Dalvit
Theoretical Division
Los Alamos National Laboratory

Collaborators

- **Theory:**

Surface-surface and atom-surface Casimir interactions

Peter Milonni (LANL)
Felipe da Rosa (now here)
Francesco Intravaia (LANL)
Ryan Behunin (LANL)
Astrid Lambrecht (LKB)
Serge Reynaud (LKB)

- **Numerics:**

Computing Casimir forces in complex nanostructures

Steven Johnson's group (MIT)
Paul Davids (Sandia)

- **Experiments:**

Measurements with AFM, MEMS, and NEMS

Toni Taylor, Igal Brener (LANL-Sandia collab.)
Ricardo Decca, Daniel Lopez (Indiana-ANL collab.)
Steve Lamoreaux (Yale)

Outline of this Talk

- Brief review of theory and experiments
- Tailoring Casimir forces with metamaterials
  - What is a metamaterial (MM)?
  - Is MM-based Casimir repulsion possible?
- Disorder in quantum vacuum
  - Casimir-induced localization of matter waves
- Thermal Casimir force
  - *First* experimental observation of the thermal Casimir force

Brief intro to Casimir physics

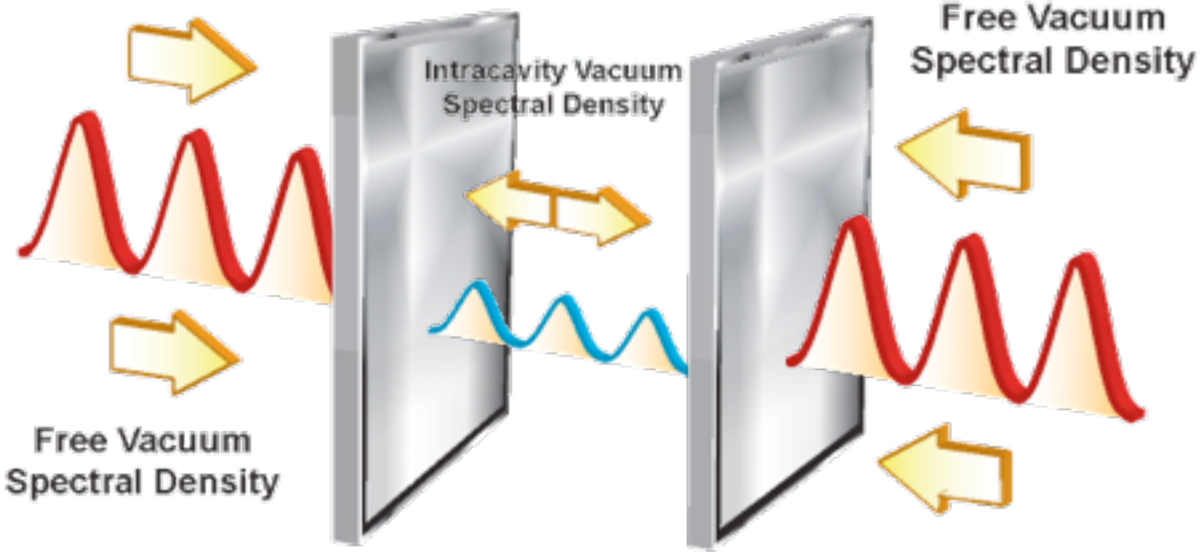

The Casimir force

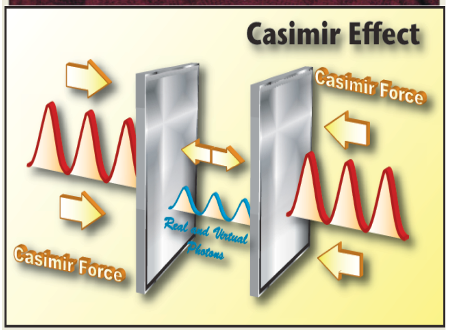

Casimir forces originate from changes in quantum vacuum fluctuations imposed by surface boundaries

They were predicted by the Dutch physicist Hendrik Casimir in 1948

$$E = \frac{1}{2}\sum_{\mathbf{k}} \hbar\omega_{\mathbf{k}} \Rightarrow \boxed{\frac{F}{A} = \frac{\pi^2}{240}\frac{\hbar c}{d^4}}$$

$$(130\mathrm{nN/cm}^2 \ @\ d = 1\mu\mathrm{m})$$

Dominant interaction in the micron and sub-micron lengthscales

The magnitude and sign of the Casimir force depend on the geometry and composition of surfaces

Modern Casimir experiments

- Torsion pendulum

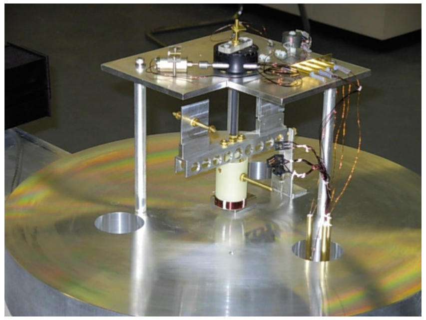

Lamoreaux

- Atomic force microscope

Onofrio, Mohideen, Iannuzzi, ...

- MEMS and NEMS

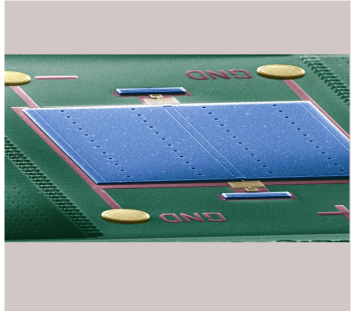

Capasso, Decca,...

- AFM/MEMS in nanostructures

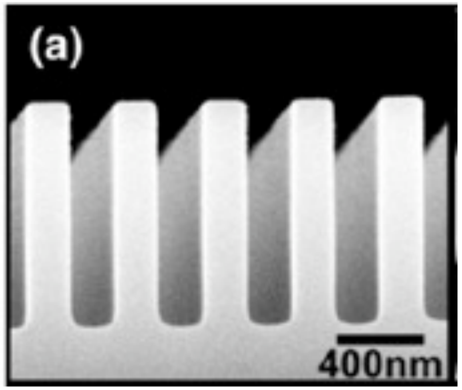

Chan, Decca

Modern Casimir experiments

- Torsion pendulum

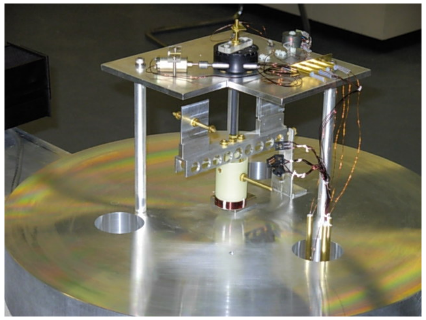

Lamoreaux

- Atomic force microscope

Onofrio, Mohideen, Iannuzzi, ...

- MEMS and NEMS

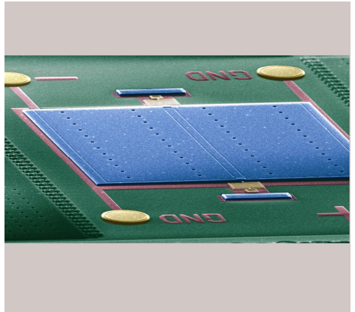

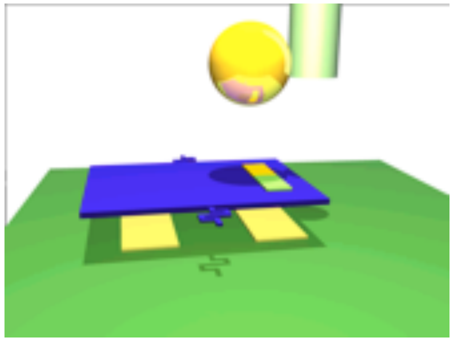

Capasso, Decca,...

- AFM/MEMS in nanostructures

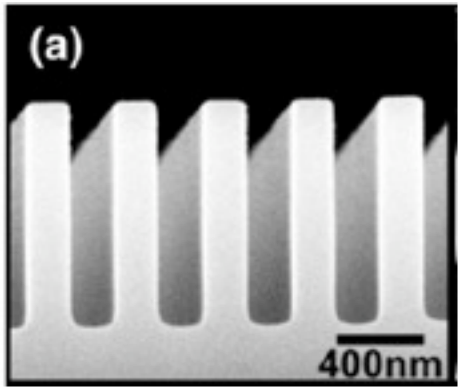

Chan, Decca

The Casimir-Polder force

vdW - CP interaction

Casimir and Polder (1948)

The interaction energy between a ground-state atom and a surface is given by

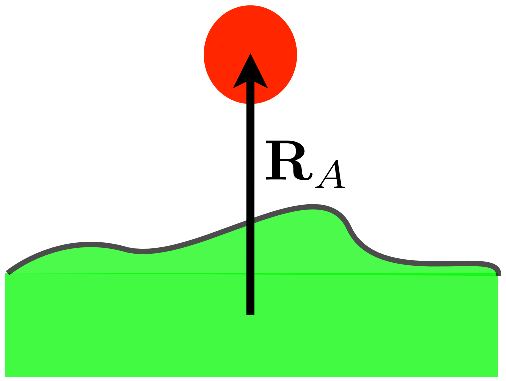

$$\boxed{U_{\mathrm{CP}}(\mathbf{R}_A) = \frac{\hbar}{c^2\epsilon_0}\int_0^\infty \frac{d\xi}{2\pi}\xi^2\alpha(i\xi)\,\mathrm{Tr}\,\mathbf{G}(\mathbf{R}_A,\mathbf{R}_A,i\xi)}$$

Atomic polarizability: $\alpha(\omega) = \lim_{\epsilon\to 0}\frac{2}{3\hbar}\sum_k \frac{\omega_{k0}|\mathbf{d}_{0k}|^2}{\omega_{k0}^2-\omega^2-i\omega\epsilon}$

Scattering Green tensor: $\left(\nabla\times\nabla\times-\frac{\omega^2}{c^2}\epsilon(\mathbf{r},\omega)\right)\mathbf{G}(\mathbf{r},\mathbf{r}',\omega)=\delta(\mathbf{r}-\mathbf{r}')$

The Casimir-Polder force

vdW - CP interaction

Casimir and Polder (1948)

The interaction energy between a ground-state atom and a surface is given by

$$\boxed{U_{\mathrm{CP}}(\mathbf{R}_A) = \frac{\hbar}{c^2\epsilon_0}\int_0^\infty \frac{d\xi}{2\pi}\xi^2\alpha(i\xi)\,\mathrm{Tr}\,\mathbf{G}(\mathbf{R}_A,\mathbf{R}_A,i\xi)}$$

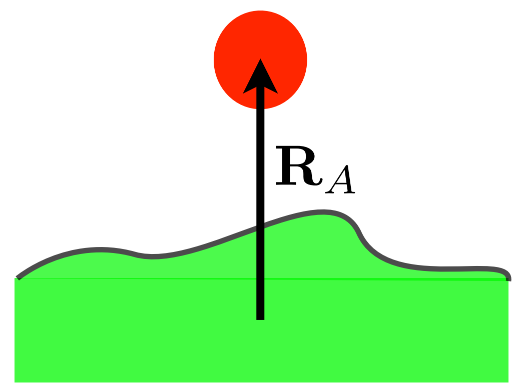

Atomic polarizability: $\alpha(\omega) = \lim_{\epsilon\to 0}\frac{2}{3\hbar}\sum_k \frac{\omega_{k0}|\mathbf{d}_{0k}|^2}{\omega_{k0}^2-\omega^2-i\omega\epsilon}$

Scattering Green tensor: $\left(\nabla\times\nabla\times-\frac{\omega^2}{c^2}\epsilon(\mathbf{r},\omega)\right)\mathbf{G}(\mathbf{r},\mathbf{r}',\omega) = \delta(\mathbf{r}-\mathbf{r}')$

Eg: Ground-state atom near planar surface @ T=0

Non-retarded (vdW) limit $z_A \ll \lambda_A$

$$U_{\mathrm{vdW}}(z_A) = -\frac{\hbar}{8\pi\epsilon_0}\frac{1}{z_A^3}\int_0^\infty \frac{d\xi}{2\pi}\alpha(i\xi)\frac{\epsilon(i\xi)-1}{\epsilon(i\xi)+1}$$

Retarded (CP) limit $z_A \gg \lambda_A$

$$U_{\mathrm{CP}}(z_A) = -\frac{3\hbar c\alpha(0)}{8\pi}\frac{1}{z_A^4}\frac{\epsilon_0-1}{\epsilon_0+1}\phi(\epsilon_0)$$

Modern CP experiments

Los Alamos NATIONAL LABORATORY

Deflection of atoms

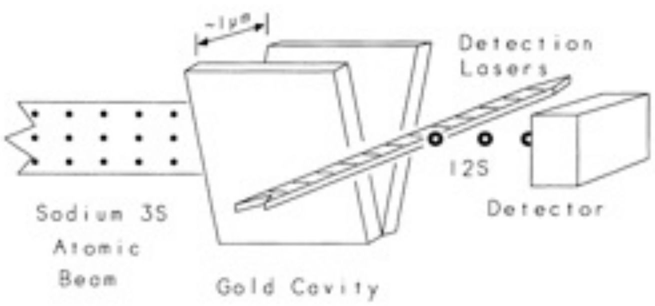

Hinds et al (1993)

Classical/quantum reflection

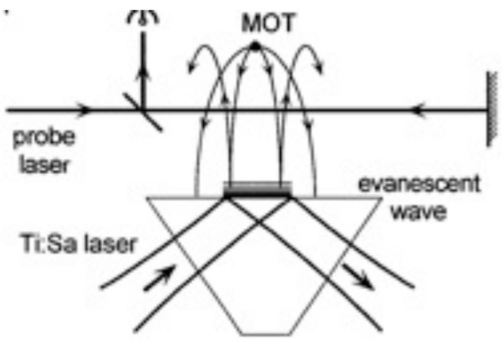

Aspect et al (1996)

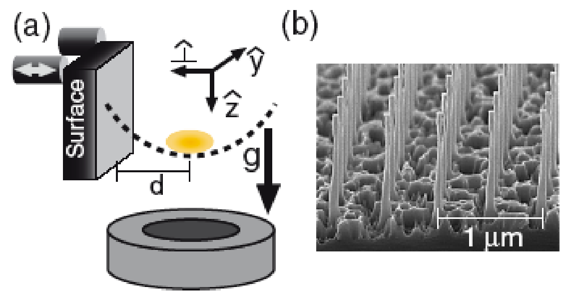

Ketterle et al (2006)

BEC oscillator

Cornell et al (2007)

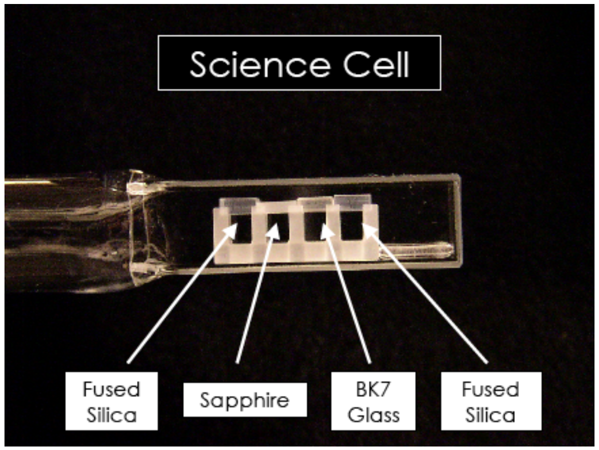

$$\gamma_x \equiv \frac{\omega_x - \omega_x'}{\omega_x} \simeq -\frac{1}{2\omega_x^2 m}\partial_x^2 U^*$$

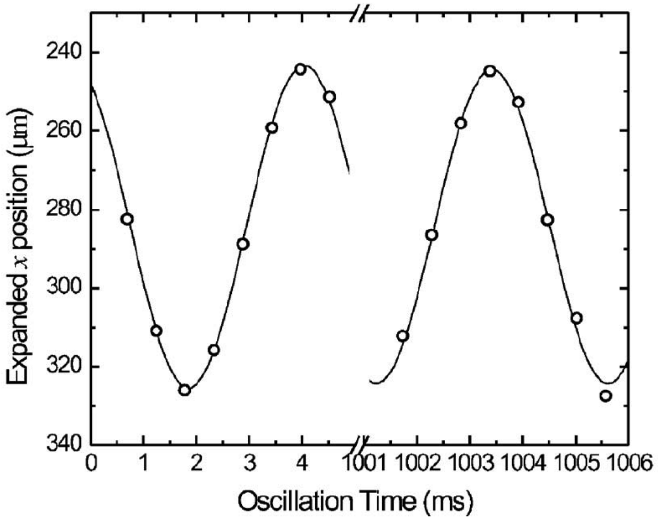

Metamaterials and Casimir

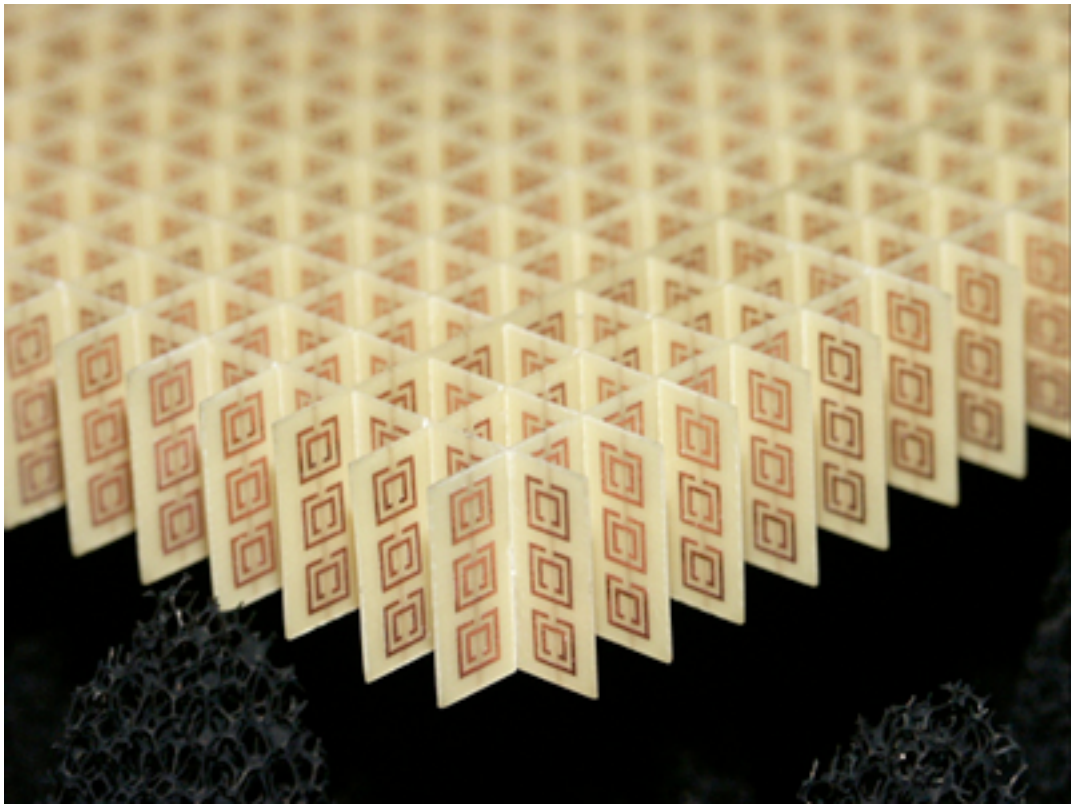

Effects of materials

The Lifshitz formula: Lifshitz (1956)

$$\boxed{\frac{F}{A} = 2\hbar\,\mathrm{Im}\int_0^\infty \frac{d\omega}{2\pi}\int\frac{d^2\mathbf{k}_\parallel}{(2\pi)^2}K_3\mathrm{Tr}\frac{\mathbf{R}_1\cdot\mathbf{R}_2 e^{2\mathrm{i}K_3 d}}{1-\mathbf{R}_1\cdot\mathbf{R}_2 e^{2\mathrm{i}K_3 d}}}$$

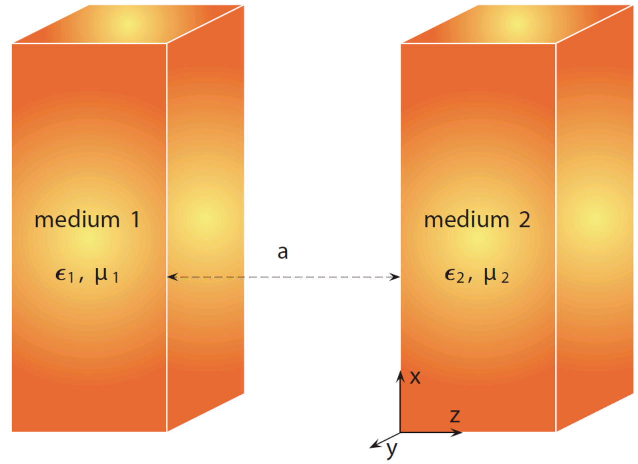

$$K_3 = \sqrt{\omega^2/c^2 - k_\parallel^2}$$

Reflection matrices (Fresnel formulas for isotropic media):

$$r^{\mathrm{TM,TM}}(\omega,\mathbf{k}_\parallel) = \frac{\epsilon(\omega)K_3 - \sqrt{\epsilon(\omega)\mu(\omega)\omega^2/c^2 - k_\parallel^2}}{\epsilon(\omega)K_3 + \sqrt{\epsilon(\omega)\mu(\omega)\omega^2/c^2 - k_\parallel^2}}$$

$r^{\mathrm{TE,TE}} = r^{\mathrm{TM,TM}}$ **with** $\epsilon \leftrightarrow \mu$

Relevant frequencies:

$$\left.\begin{array}{lll} \epsilon(\omega) \xrightarrow{\omega\gg\Omega_p} 1 & \Rightarrow & r^{p,p}\approx 0 \text{ (Transparent plates)} \\ \omega \gg c/d & \Rightarrow & e^{2\mathrm{i}K_3 d}\approx 0 \text{ (Fast oscillations)} \end{array}\right\} \Rightarrow F\approx 0$$

$$\boxed{0 \le \omega \le \min\{\Omega_p, c/d\}}$$

Going to imaginary frequencies

$$\frac{F}{A} = 2\hbar \int_0^\infty \frac{d\xi}{2\pi} \int \frac{d^2\mathbf{k}_\parallel}{(2\pi)^2} K_3 \mathrm{Tr} \frac{\mathbf{R}_1 \cdot \mathbf{R}_2 e^{-2K_3 d}}{1 - \mathbf{R}_1 \cdot \mathbf{R}_2 e^{-2K_3 d}}$$

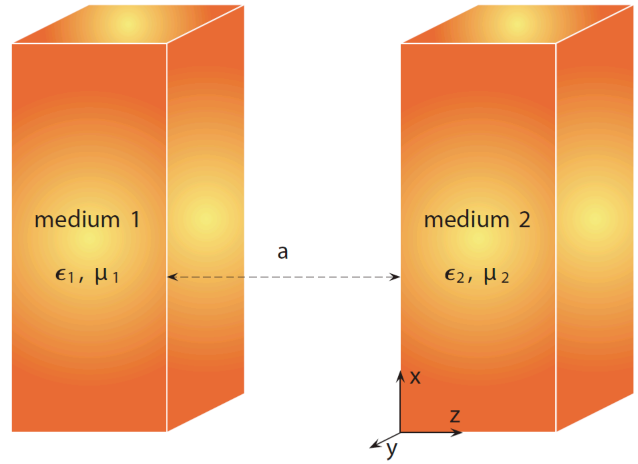

Kramers-Kronig (causality) relations:

$$\epsilon(i\xi) = 1 + \frac{2}{\pi} \int_0^\infty \frac{\omega \epsilon''(\omega)}{\omega^2 + \xi^2} d\omega \qquad \mu(i\xi) = 1 + \frac{2}{\pi} \int_0^\infty \frac{\omega \mu''(\omega)}{\omega^2 + \xi^2} d\omega$$

Dominant frequencies below the near-infrared/optical region of the EM spectrum (gaps d= 200-1000 nm)

The important message is that Casimir is a broad-band frequency phenomenon

The sign of the Casimir force

Los Alamos NATIONAL LABORATORY

$$\frac{F}{A} = 2\hbar \int_0^\infty \frac{d\xi}{2\pi} \int \frac{d^2\mathbf{k}_\parallel}{(2\pi)^2} K_3 \mathrm{Tr} \frac{\mathbf{R}_1 \cdot \mathbf{R}_2 e^{-2K_3 d}}{1 - \mathbf{R}_1 \cdot \mathbf{R}_2 e^{-2K_3 d}}$$

The sign of the force is directly connected to the sign of the product of the reflection coefficients on the two plates, evaluated at imaginary frequencies. As a rule of thumb, we have (p=TE, TM)

$$R_1^p(i\xi) \cdot R_2^p(i\xi) > 0 \ (\forall\, \xi \leq c/d) \Rightarrow \text{Attraction}$$

$$R_1^p(i\xi) \cdot R_2^p(i\xi) < 0 \ (\forall\, \xi \leq c/d) \Rightarrow \text{Repulsion}$$

In terms of permittivities and permeabilities:

$$\left.\begin{array}{l} \epsilon_a(i\xi) \gg \epsilon_b(i\xi) \\ \mu_b(i\xi) \gg \mu_a(i\xi) \end{array}\right. \longrightarrow \text{Repulsion}$$

Ideal attraction-repulsion

- **Ideal attractive limit**

  Casimir (1948)

$$\boxed{\frac{F}{A} = +\frac{\pi^2}{240}\frac{\hbar c}{d^4}}$$

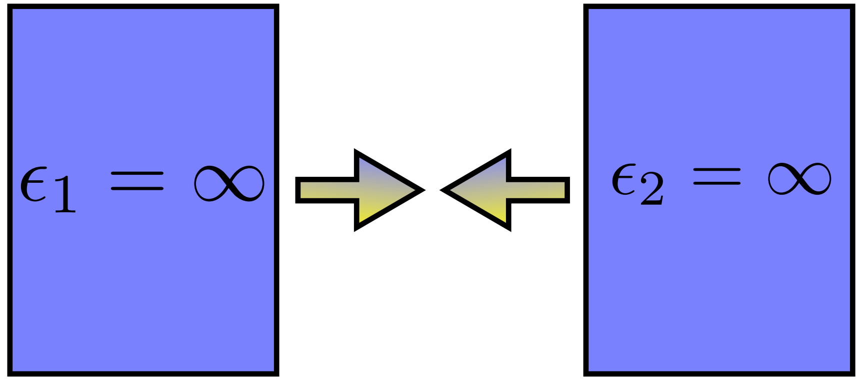

Ideal attraction-repulsion

- **Ideal attractive limit**

  Casimir (1948)

$$\boxed{\frac{F}{A} = +\frac{\pi^2}{240}\frac{\hbar c}{d^4}}$$

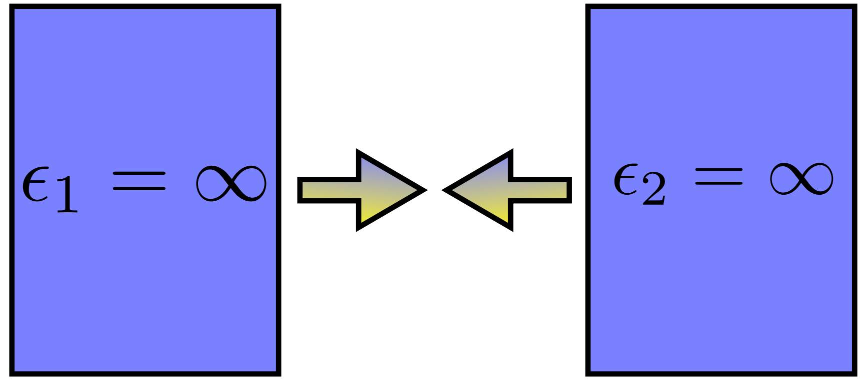

- **Ideal repulsive limit**

  Boyer (1974)

$$\boxed{\frac{F}{A} = -\frac{7}{8}\frac{\pi^2}{240}\frac{\hbar c}{d^4}}$$

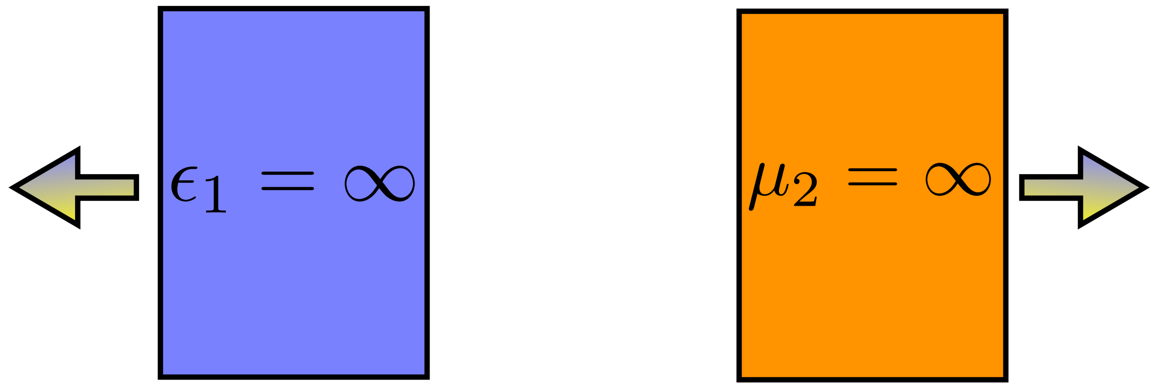

Ideal attraction-repulsion

- **Ideal attractive limit**

  Casimir (1948)

$$\boxed{\frac{F}{A} = +\frac{\pi^2}{240}\frac{\hbar c}{d^4}}$$

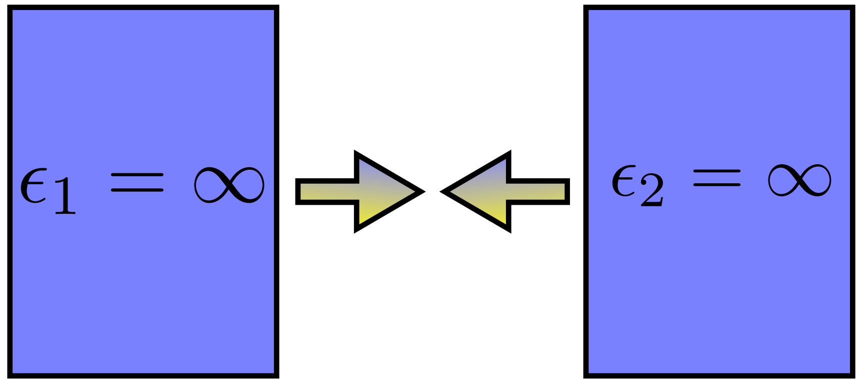

- **Ideal repulsive limit**

  Boyer (1974)

$$\boxed{\frac{F}{A} = -\frac{7}{8}\frac{\pi^2}{240}\frac{\hbar c}{d^4}}$$

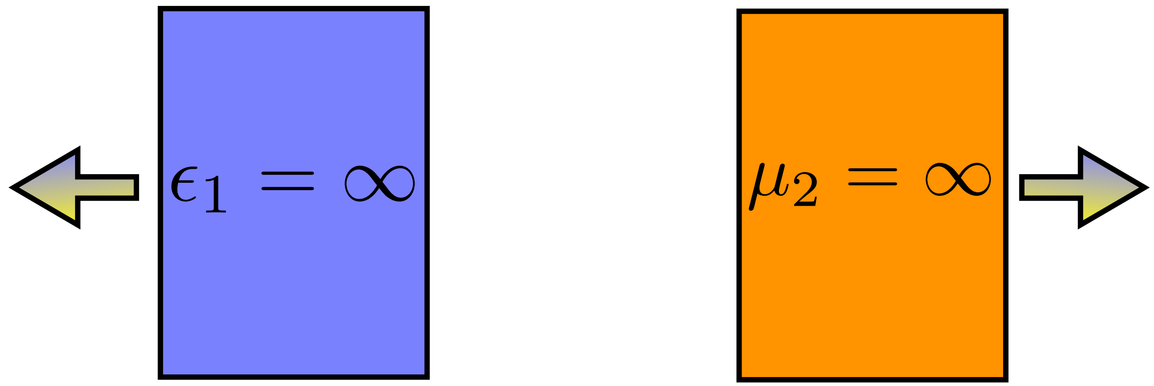

- **Real repulsive limit**

  Casimir repulsion is associated with strong electric-magnetic interactions. However, natural occurring materials do NOT have strong magnetic response in the optical region, i.e. $\mu = 1$

Ideal attraction-repulsion

Ideal attractive limit

Casimir (1948)

$$\boxed{\frac{F}{A} = +\frac{\pi^2}{240}\frac{\hbar c}{d^4}}$$

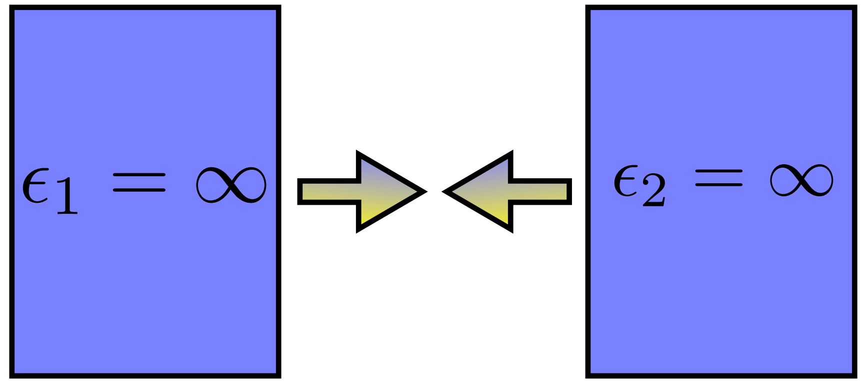

Ideal repulsive limit

Boyer (1974)

$$\boxed{\frac{F}{A} = -\frac{7}{8}\frac{\pi^2}{240}\frac{\hbar c}{d^4}}$$

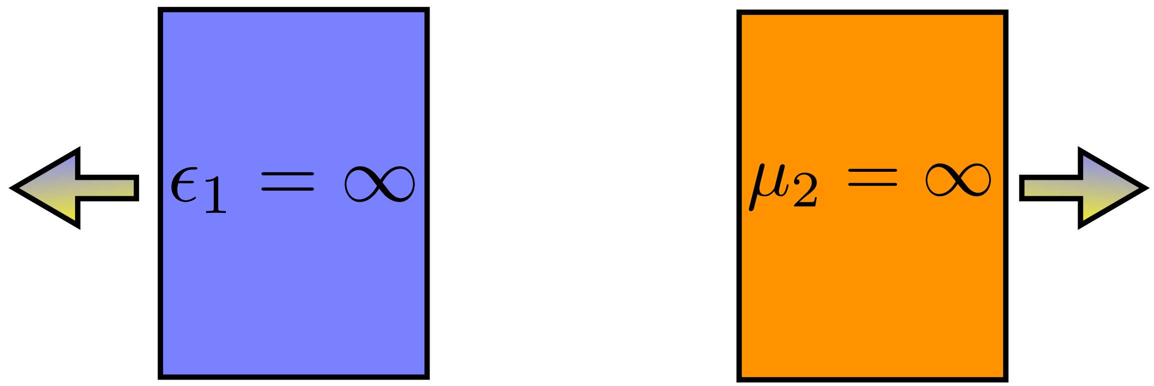

Real repulsive limit

Casimir repulsion is associated with strong electric-magnetic interactions. However, natural occurring materials do NOT have strong magnetic response in the optical region, i.e. $\mu = 1$ → **Metamaterials**

Quantum levitation with MMs?

Los Alamos NATIONAL LABORATORY

Physicists have 'solved' mystery of levitation

By Roger Highfield, Science Editor
Last Updated: 1:41am BST 08/08/2007

Levitation has been elevated from being pure science fiction to science fact, according to a study reported today by physicists.

In earlier work the same team of theoretical physicists showed that invisibility cloaks are feasible.

Now, in another report that sounds like it comes out of the pages of a Harry Potter book, the University of St Andrews team has created an 'incredible levitation effects' by engineering the force of nature which normally causes objects to stick together.

Professor Ulf Leonhardt and Dr Thomas Philbin, from the University of St Andrews in Scotland, have worked out a way of reversing this phenomenon, known as the Casimir force, so that it repels instead of attracts.

Their discovery could ultimately lead to frictionless micro-machines with moving parts that levitate But they say that, in principle at least, the same effect could be used to levitate bigger objects too, even a person.

In theory the discovery could be used to levitate a person

The Casimir force is a consequence of quantum mechanics, the theory that describes the world of atoms and subatomic particles that is not only the most successful theory of physics but also the most baffling.

The force is due to neither electrical charge or gravity, for example, but the fluctuations in all-pervasive energy fields in the intervening empty space between the objects and is one reason atoms stick together, also explaining a "dry glue" effect that enables a gecko to walk across a ceiling.

Now, using a special lens of a kind that has already been built, Prof Ulf Leonhardt and Dr Thomas Philbin report in the New Journal of Physics they can engineer the Casimir force to repel, rather than attact.

Because the Casimir force causes problems for nanotechnologists, who are trying to build electrical circuits and tiny mechanical devices on silicon chips, among other things, the team believes the feat could initially be used to stop tiny objects from sticking to each other.

Prof Leonhardt explained, "The Casimir force is the ultimate cause of friction in the nano-world, in particular in some microelectromechanical systems.

Such systems already play an important role - for example tiny mechanical devices which triggers a car airbag to inflate or those which power tiny 'lab on chip' devices used for drugs testing or chemical analysis.

Micro or nano machines could run smoother and with less or no friction at all if one can manipulate the force." Though it is possible to levitate objects as big as humans, scientists are a long way off developing the technology for such feats, said Dr Philbin.

The practicalities of designing the lens to do this are daunting but not impossible and levitation "could happen over quite a distance".

Prof Leonhardt leads one of four teams - three of them in Britain - to have put forward a theory in a peer-reviewed journal to achieve invisibility by making light waves flow around an object - just as a river flows undisturbed around a smooth rock.

Print | Email this story

Post this story to: del.icio.us | Digg | Newsvine | NowPublic | Reddit

"In theory the discovery could be used to levitate a person"

Metamaterials

Los Alamos
NATIONAL LABORATORY

- Artificial structured composites with designer electromagnetic properties
- MMs are strongly anisotropic, dispersive, magneto-dielectric media.

Negative refraction	Veselago (1968), Smith et al (2000)
Perfect lens	Pendry (2000)
Cloaking	Smith et al (2007)

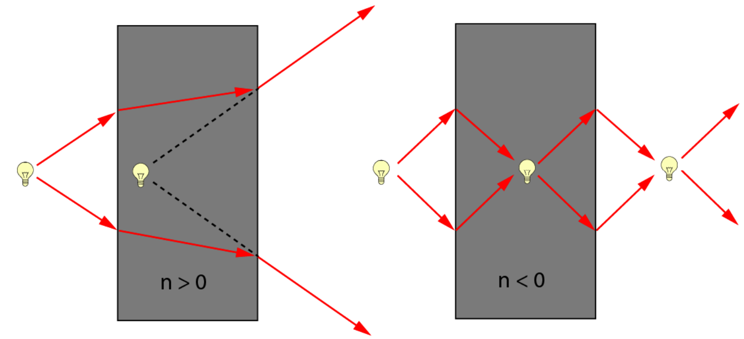

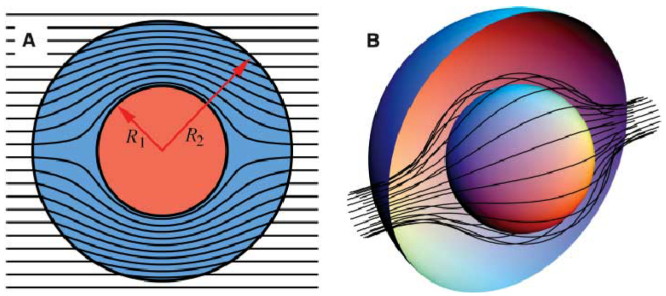

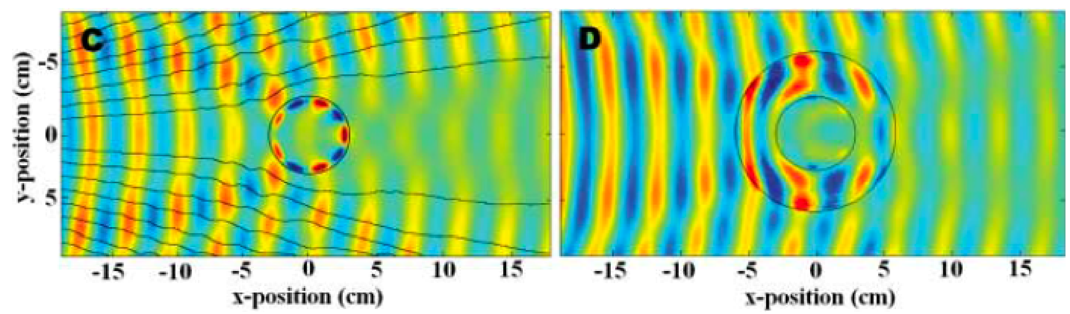

THz MMs: eg split ring resonators

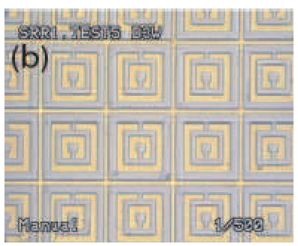

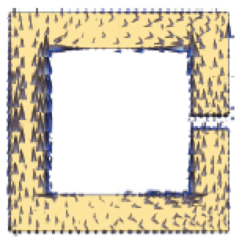

36μm

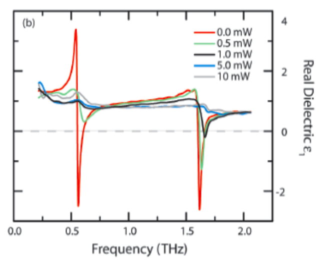

$\epsilon, \mu < 0$

Optical MMs: eg nano-pillars

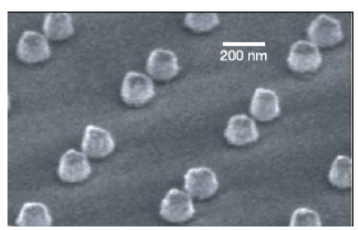

200nm

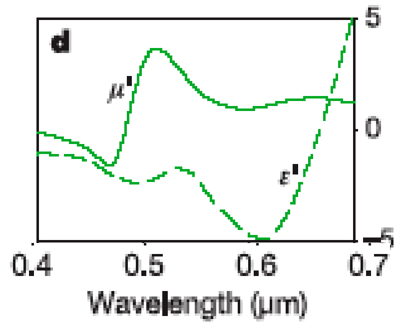

Effective medium approximation

We want to compute the Casimir force between a metallic plate and a MM. Let us assume a metallic plate in is reasonably well described by a Drude response

$$\epsilon_1(\omega) = 1 - \frac{\Omega_e^2}{\omega^2 + i\gamma_e\omega} \qquad \mu_1 = 1$$

For the MM the optical response is not so simple.....

In the effective medium approximation (EMA) one describes the MM with an effective electric permittivity and an effective magnetic permeability. This is an approximation valid when the MM is probed at wavelengths much larger that the average distance between the constituent "particles" of the MM.

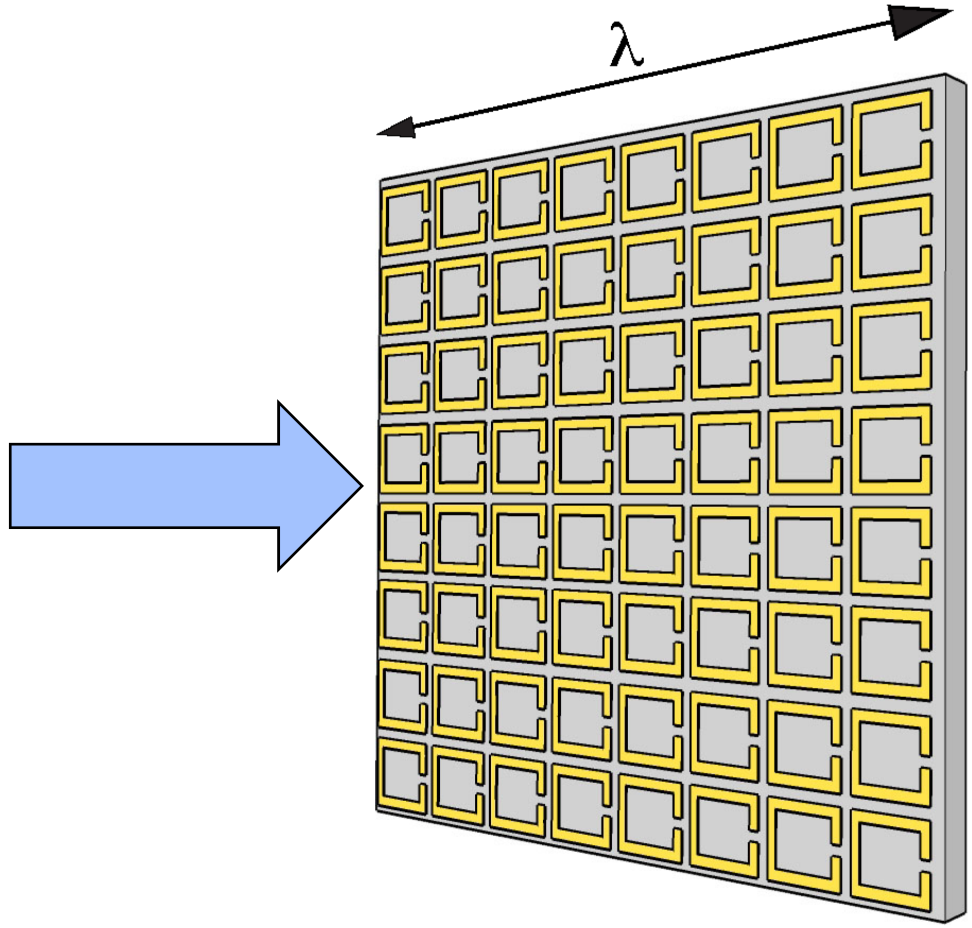

EMA: Electric response

Close to resonance, the optical response can be modeled by a Drude-Lorentz permittivity

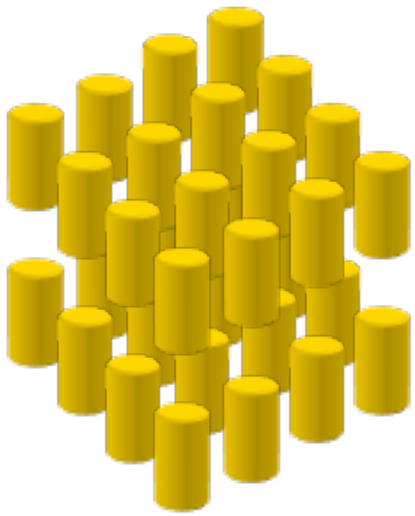

$$\varepsilon(\omega) = 1 - \frac{\omega_p^2 - \omega_0^2}{\omega^2 - \omega_0^2 + i\omega\Gamma}$$

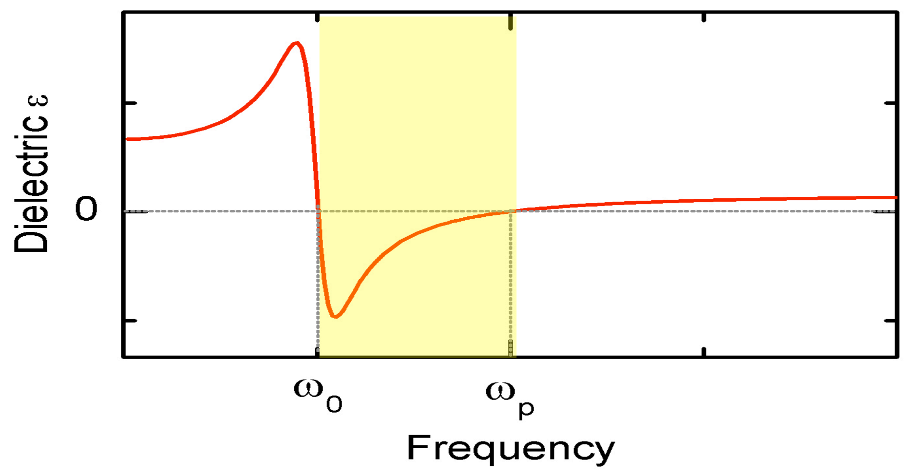

J.B. Pendry ***et al.*, *Phys. Rev. Lett.* 76**, 4773 (1996).

EMA: Magnetic response

$$\mu_{eff} = 1 - \frac{\frac{\pi r^2}{a^2}}{1 + \frac{2\sigma i}{\omega r \mu_0} - \frac{3}{\pi^2 \mu_0 \omega^2 C r^3}}$$

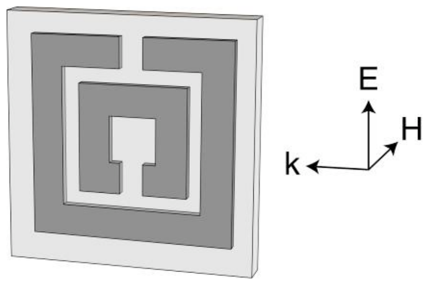

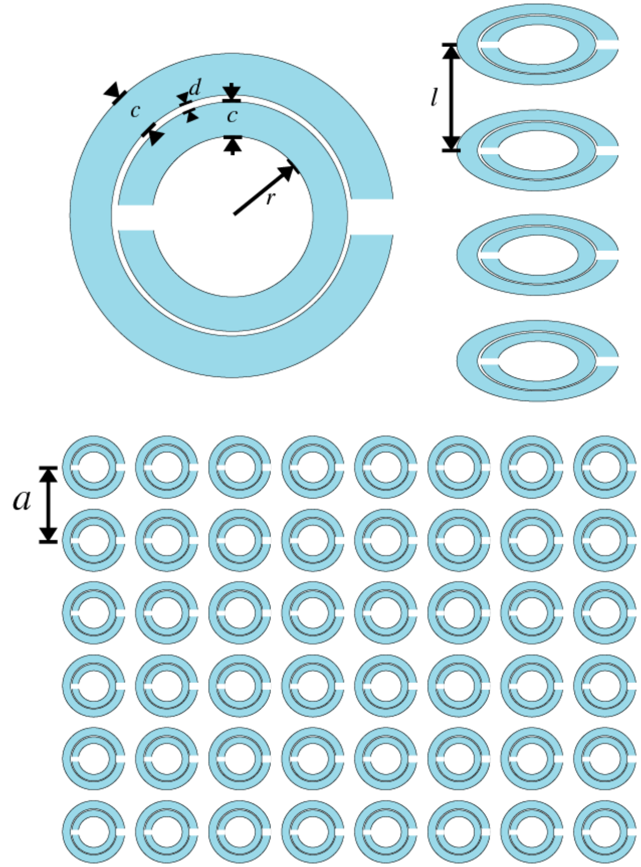

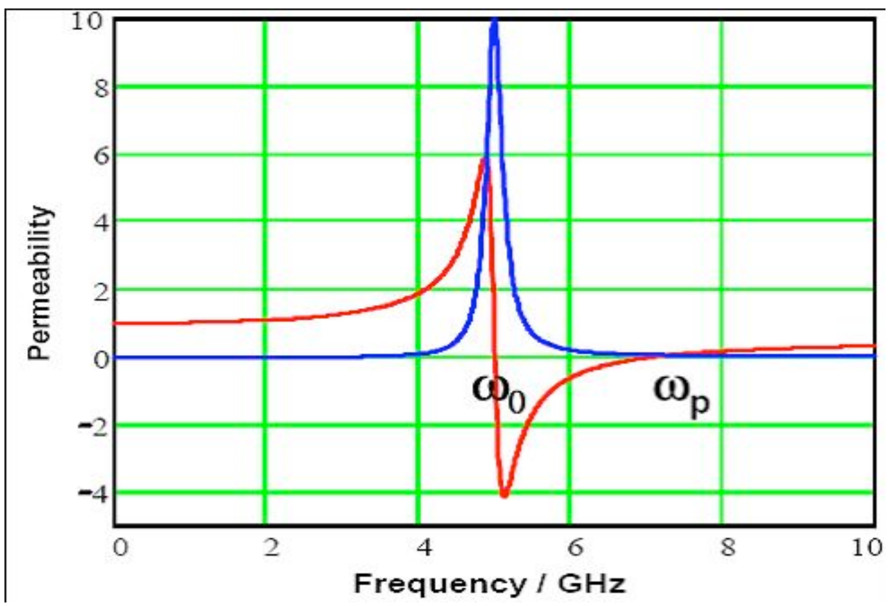

J.B. Pendry *et al.*, *IEEE Trans. Microwave Tech.* **47,** 2075 (1999).

EMA: Drude-Lorentz responses

Close to the resonance, both $\epsilon(\omega)$ and $\mu(\omega)$ can be modeled by Drude-Lorentz formulas

$$\epsilon_\alpha(\omega) = 1 - \frac{\Omega^2_{E,\alpha}}{\omega^2 - \omega^2_{E,\alpha} + i\Gamma_{E,\alpha}\omega}$$

$$\mu_\alpha(\omega) = 1 - \frac{\Omega^2_{M,\alpha}}{\omega^2 - \omega^2_{M,\alpha} + i\Gamma_{M,\alpha}\omega}$$

Typical separations

$$d = 200 - 1000 \text{ nm}$$

Infrared-optical frequencies

$$\Omega/2\pi = 5 \times 10^{14}\text{Hz}$$

Drude metal (Au)

$\Omega_E = 9.0 \text{ eV} \quad \Gamma_E = 35 \text{ meV}$

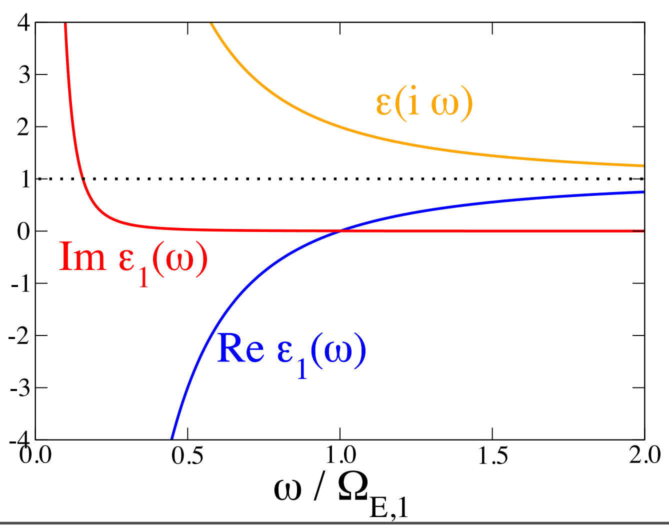

Metamaterial

$\text{Re } \epsilon_2(\omega) < 0 \quad \text{Re } \mu_2(\omega) < 0$

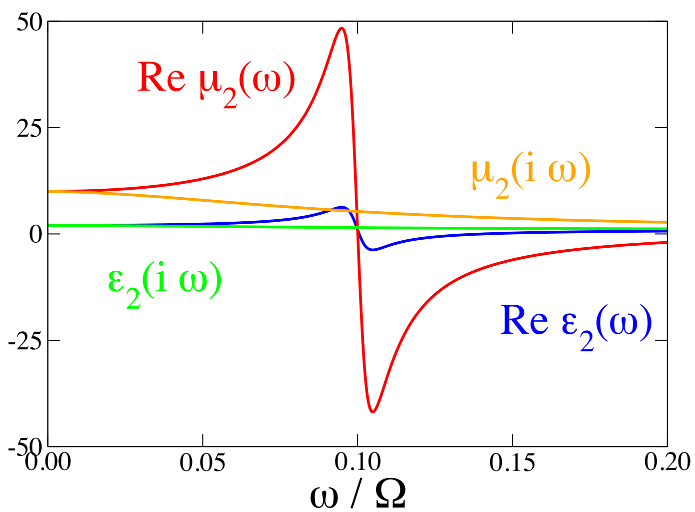

$$\Omega_{E,2}/\Omega = 0.1 \quad \Omega_{M,2}/\Omega = 0.3$$

$$\omega_{E,2}/\Omega = \omega_{M,2}/\Omega = 0.1$$

$$\Gamma_{E,2}/\Omega = \Gamma_{M,2}/\Omega = 0.01$$

Attraction-repulsion crossover

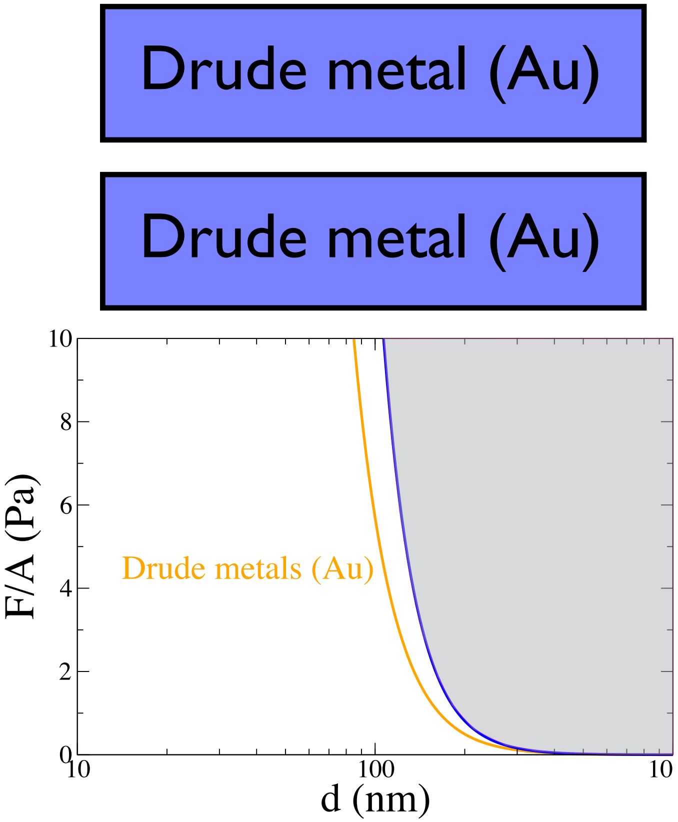

Only attraction

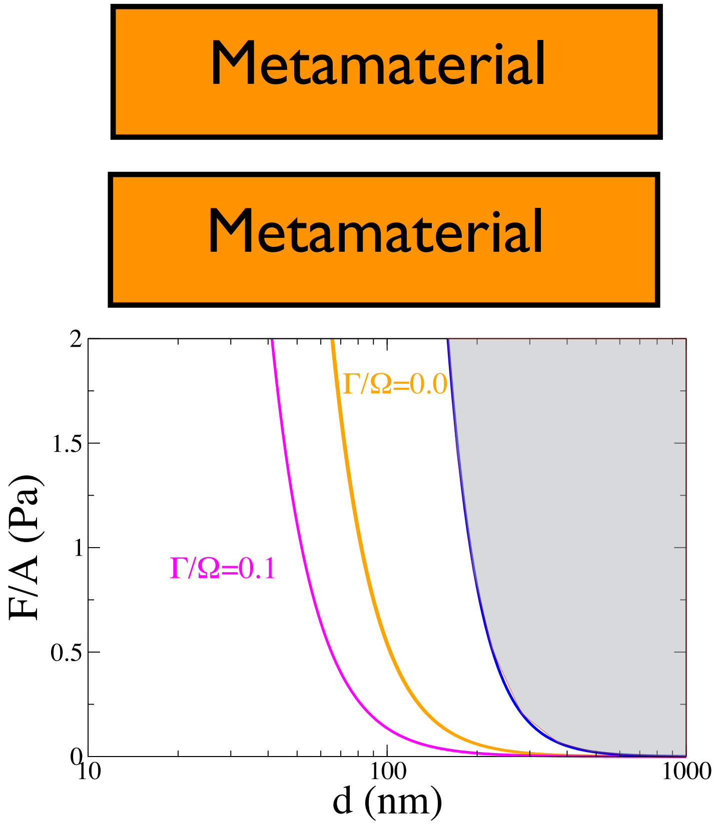

Only attraction

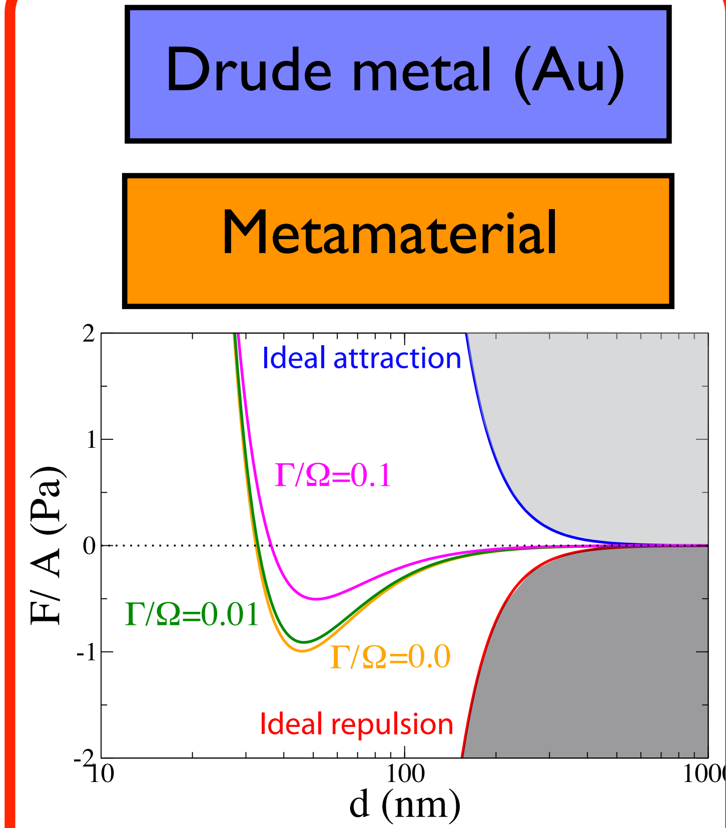

Repulsion-attraction

Drude background

- In some metallic-based MMs, there is a net conductivity due to the metallic structure, like the fishnet design on the right.

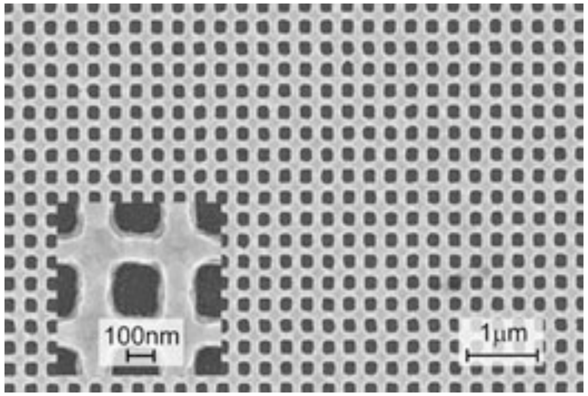

$$\epsilon(\omega) = 1 - f\frac{\Omega_D^2}{\omega^2 - i\omega\gamma_D} - (1-f)\frac{\Omega_e^2}{\omega^2 - \omega_e^2 + i\gamma_e\omega}$$

f : filling factor

$$\mu(\omega) = 1 - \frac{\Omega_m^2}{\omega^2 - \omega_m^2 + i\gamma_m\omega}$$

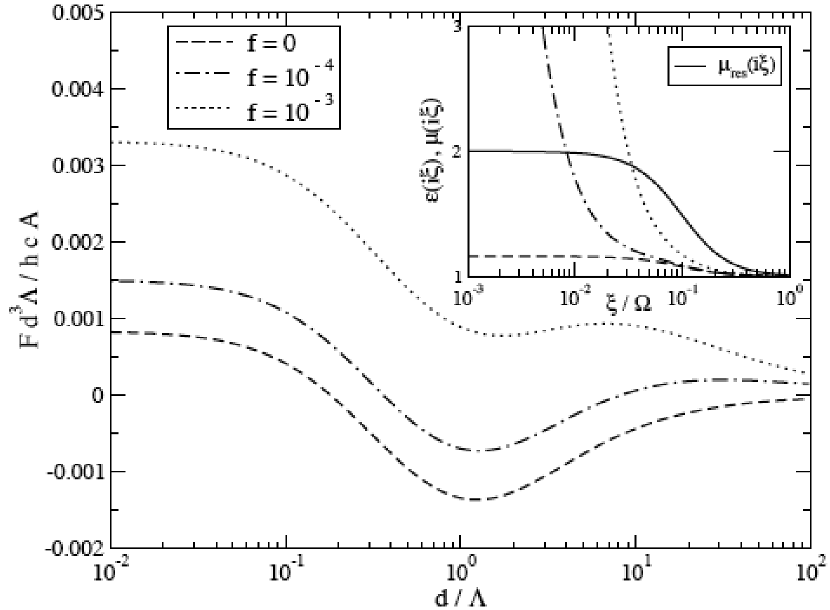

Rosa, DD, Milonni, PRL 2008

A Drude background is detrimental for Casimir force reduction or repulsion, since it results in an electric response much stronger than the magnetic one

$$\epsilon_2(i\xi) \gg \mu_2(i\xi)$$

EMA: correct model for μ

Drude-Lorentz for permeability is wrong. The correct expression that results in EMA from Maxwell's equations is

$$\boxed{\mu_{\text{eff}}(\omega) = 1 - f\frac{\omega^2}{\omega^2 - \omega_m^2 + 2i\gamma_m\omega}}$$

(Pendry 1999)

The appearance of the ω^2 factor in the numerator is very important:

Although close to the resonance this behaves in the same way as the Drude-Lorentz EMA permeability, it has a completely different low-frequency behavior

$$\mu_{\text{eff}}(i\xi) < 1 < \epsilon_{\text{eff}}(i\xi)$$

No Casimir repulsion!

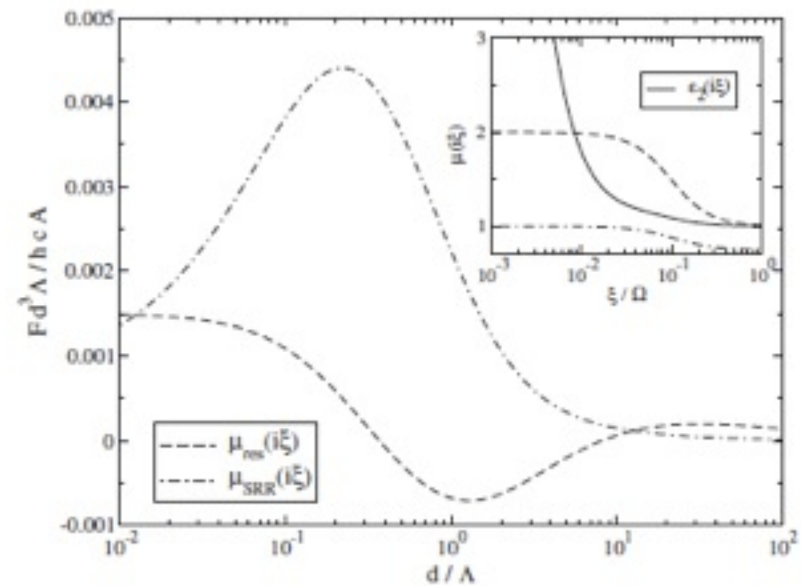

Other Casimir MMs: chirality

Los Alamos NATIONAL LABORATORY

The chirality of a MM is defined by the chirality of its unit cell

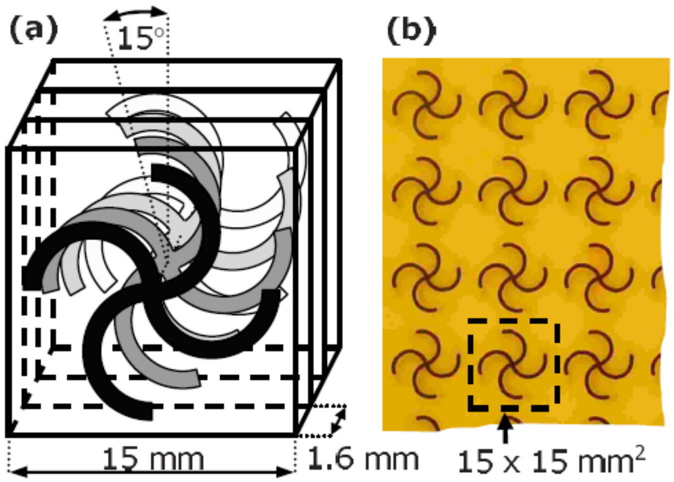

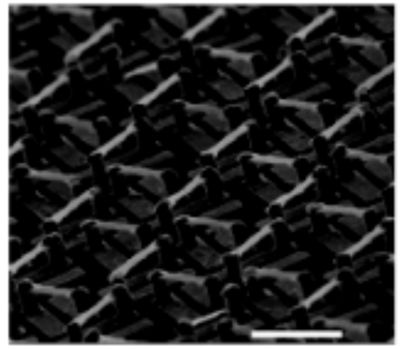

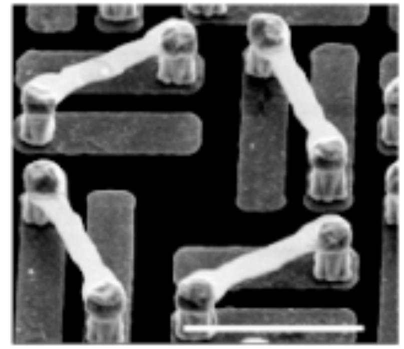

In a chiral medium, the constitutive relations mix electric and magnetic fields

$$\mathbf{D}(\mathbf{r},\omega) = \epsilon(\omega)\mathbf{E}(\mathbf{r},\omega) - i\kappa(\omega)\mathbf{H}(\mathbf{r},\omega)$$
$$\mathbf{B}(\mathbf{r},\omega) = i\kappa(\omega)\mathbf{E}(\mathbf{r},\omega) + \mu(\omega)\mathbf{H}(\mathbf{r},\omega)$$

dispersive chirality: $\kappa(\omega) = \dfrac{\omega_k \omega}{\omega^2 - \omega_{\kappa R}^2 + i\gamma_k \omega}$

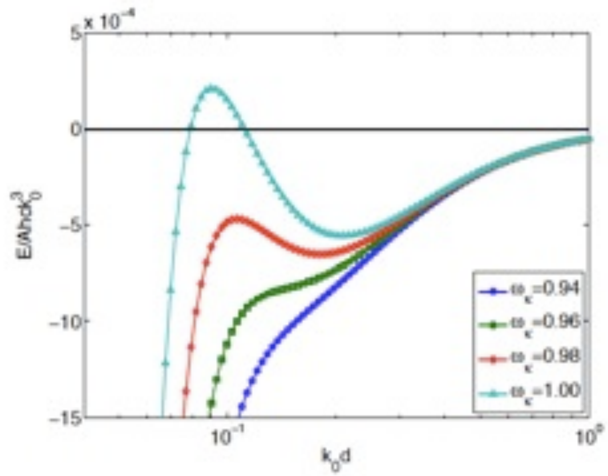

Same-chirality (SC) materials: repulsion

Opposite-chirality (OC) materials: attraction

Soukoulis et al, PRL 2009

Beyond EMA

Los Alamos NATIONAL LABORATORY

Everything discussed so far is based on the assumption that the effective medium approximation (EMA) holds. We recall that this amounts to treating the MM in the "long-wavelength approximation", i.e., field wavelengths much larger than the typical size of the unit cell of the MM.

How to calculate Casimir forces when EMA does not hold?
Can one trust predictions of Casimir repulsion with MMs based on EMA?

Homogeneous medium | Non-homogeneous medium

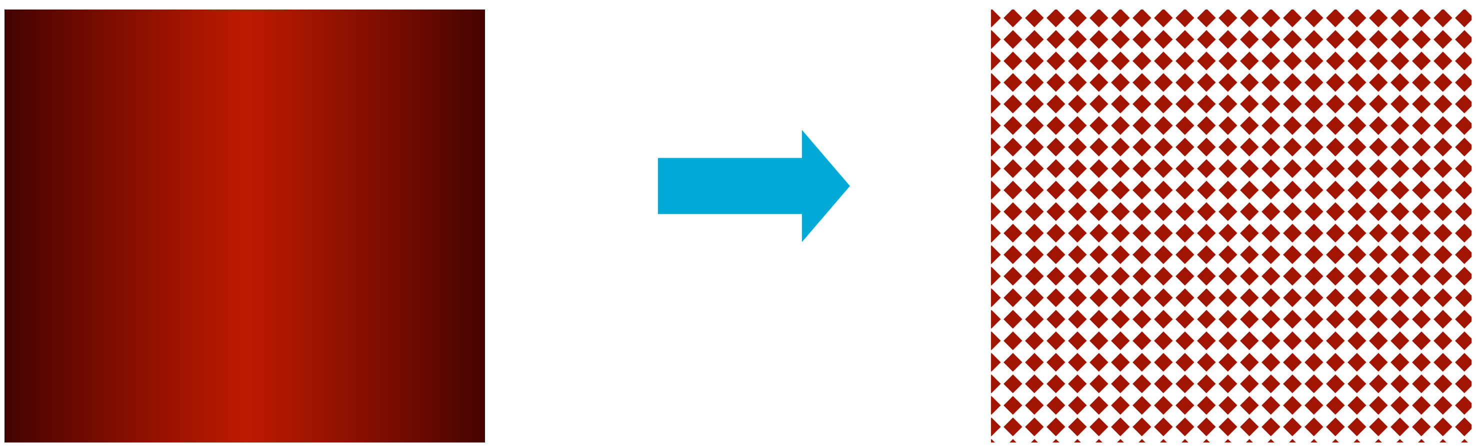

EMA | beyond EMA

Exact method: Scattering theory

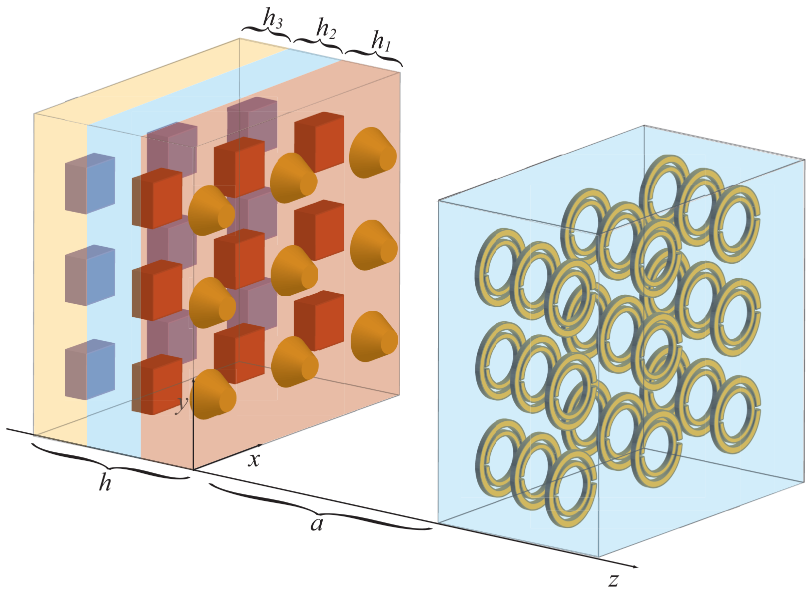

The Casimir force still may be described in terms of reflections (scattering theory)

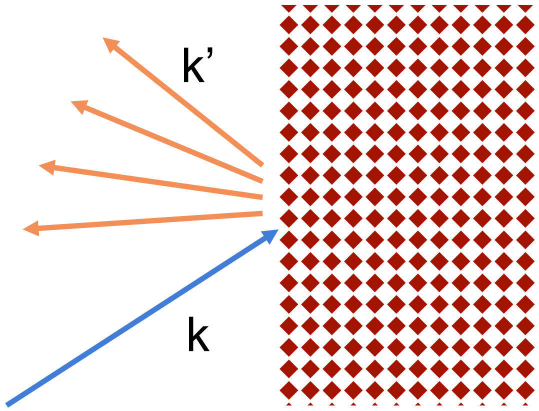

Symbolically, we may write the Casimir energy as

$$\boxed{\frac{E(d)}{A} = \hbar \int_0^\infty \frac{d\xi}{2\pi} \log\det\left[1 - \mathcal{R}_1 e^{-\mathcal{K}d} \mathcal{R}_2 e^{-\mathcal{K}d}\right]}$$

where $\quad \mathcal{R}_i \equiv \mathcal{R}_i(\mathbf{k}_{||}, \mathbf{k}'_{||}, p, p', i\xi)$

Solving for the reflection matrix

The reflection matrix can be obtained with standard methods of numerical electromagnetism. One way is to solve Maxwell equations for the transverse fields

$$-ik\frac{\partial \mathbf{E}_t}{\partial z} = \nabla_t\left[\chi\hat{e}_3\cdot\nabla\times\mathbf{H}_t\right] - k^2\mu\hat{e}_3\times\mathbf{H}_t$$
$$-ik\frac{\partial \mathbf{H}_t}{\partial z} = -\nabla_t\left[\zeta\hat{e}_3\cdot\nabla\times\mathbf{E}_t\right] + k^2\epsilon\hat{e}_3\times\mathbf{E}_t$$

Assuming a two-dimensional periodic structure, we have

$$\mathbf{E}_t(x,y) = e^{i\mathbf{k}\cdot\mathbf{r}}\sum_{m,n}\mathcal{E}_{m,n}\ \exp\left[i\frac{2\pi n}{L_x}x + i\frac{2\pi m}{L_y}y\right]$$
$$\mathbf{H}_t(x,y) = e^{i\mathbf{k}\cdot\mathbf{r}}\sum_{m,n}\mathcal{H}_{m,n}\ \exp\left[i\frac{2\pi n}{L_x}x + i\frac{2\pi m}{L_y}y\right]$$

where

$$\epsilon(x,y) = \sum_{m,n}\epsilon_{m,n}\ \exp\left[i\frac{2\pi n}{L_x}x + i\frac{2\pi m}{L_y}y\right]$$
$$\mu(x,y) = \sum_{m,n}\mu_{m,n}\ \exp\left[i\frac{2\pi n}{L_x}x + i\frac{2\pi m}{L_y}y\right]$$

Exact reflection matrix

One can then write the equations for the transverse fields as

$$\boxed{-ik\frac{\partial \mathbf{\Psi}_{m'n'}}{\partial z} = \sum_{mn} H_{m'n',mn}\mathbf{\Psi}_{mn}} \qquad \mathbf{\Psi}_{mn} = \begin{bmatrix} \mathcal{E}^x_{mn} \\ \mathcal{E}^y_{mn} \\ \mathcal{H}^x_{mn} \\ \mathcal{E}^y_{mn} \end{bmatrix} = \begin{bmatrix} \Psi^1_{mn} \\ \Psi^2_{mn} \\ \Psi^3_{mn} \\ \Psi^4_{mn} \end{bmatrix}$$

Here H is a complicated matrix, that encapsulated the coupling of modes in the periodic structure.

By numerically solving this equation and imposing the proper boundary conditions of the field on the vacuum-metamaterial interphase (RCWA or S-matrix techniques), one can find the reflection matrix of the MM.

2D periodic structures - finite T

Casimir force between a Au sphere and Si pillars/grating/membrane @ T=300 K

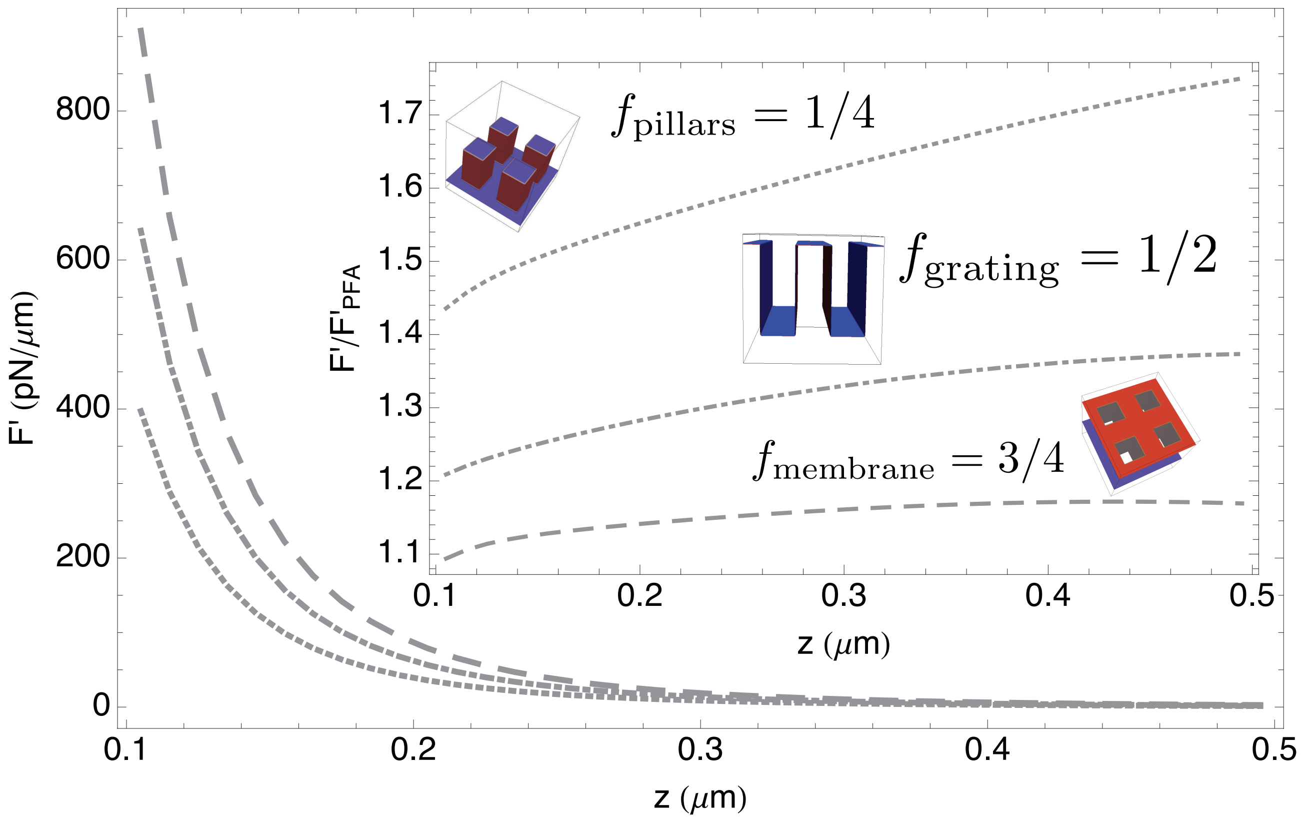

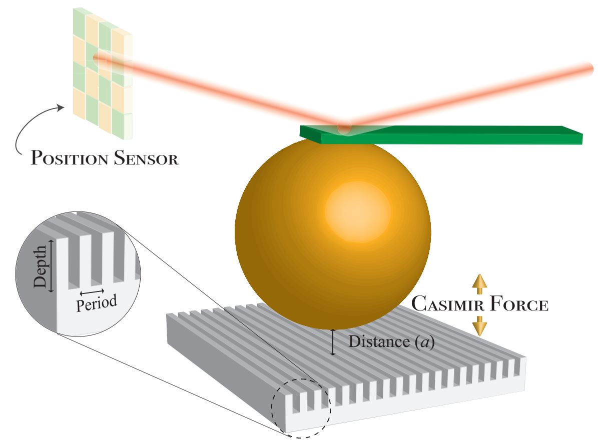

$$R = 50\mu\mathrm{m}$$

$$\mathrm{period} = 400\ \mathrm{nm}$$

$$\mathrm{depth} = 1070\ \mathrm{nm}$$

Davids, Intravaia, Rosa, DD, arXiv:1008.3580 (to appear in PRA)

Chiral MMs. I

Configurations

No difference in metamaterial approx.

Unit Cell

Aligned

Shifted

Chirality

(SC)

(OC)

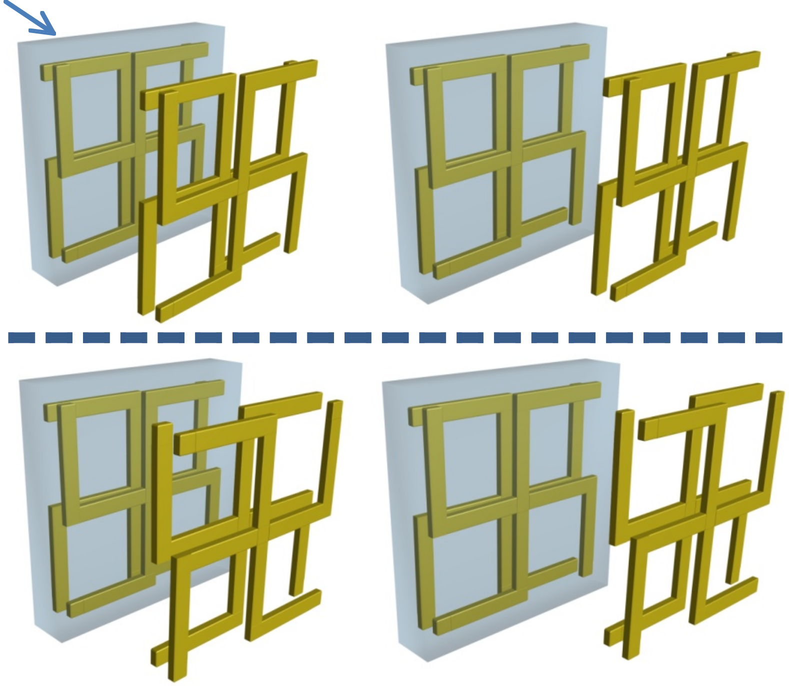

Attractive, $F_{OC} > F_{SC}$ in metamaterial limit

Results

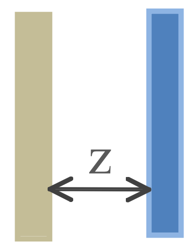

Force F in SC and OC configs.

Plot $(F_{OC} - F_{SC}) / F_{OC}$:

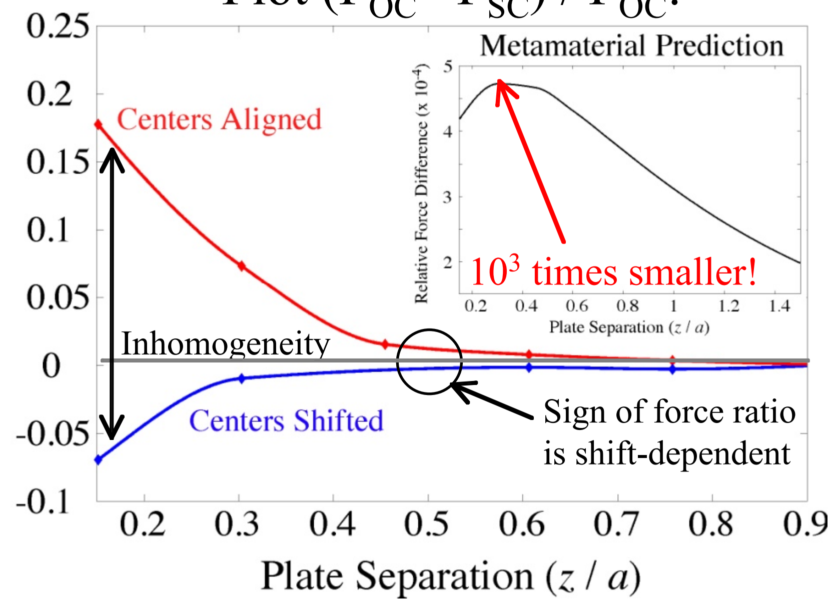

McCauley et al, PRB 2010

Chiral MMs. II

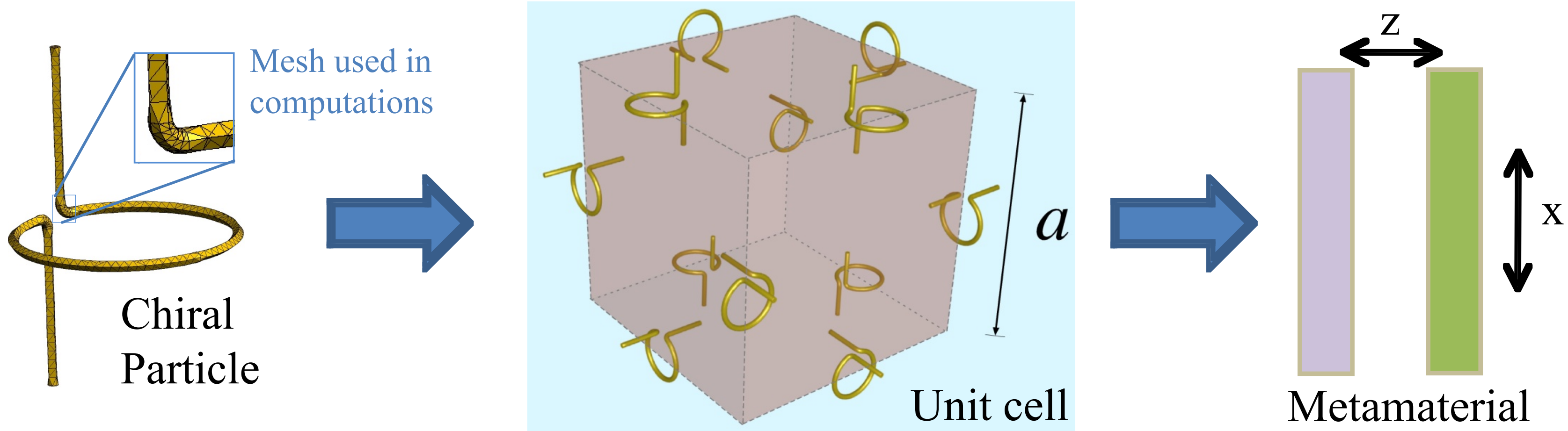

Effect of inhomogeneity across displacements x

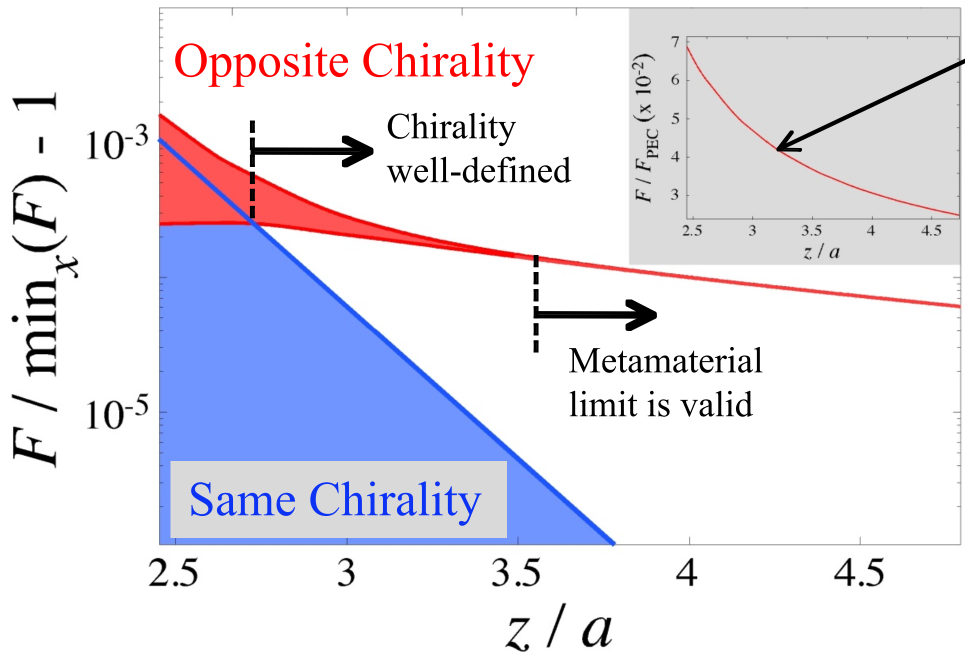

Total force relative to parallel metal plates

"repulsive" effect (force reduction) of chirality is one ten-thousandth of this!

Conclusion

In the regime where the chiral metamaterial limit is valid, the effect is **too small** to be observable.

McCauley et al, PRB 2010

Remarks: MMs and Casimir

- Metamaterials offer an interesting possibility for Casimir force manipulation: engineered optical response, (maybe) broadband, dynamic control.

- Several proposals for MM-based Casimir force use effective medium approximation. Their predictions have to be carefully checked since EMA breaks down for electromagnetic fluctuations with wavelengths comparable to metamaterial feature sizes.

- Casimir repulsion in vacuum-separated metallic/dielectric metamaterial structures seems hard to achieve. It is certainly impossible in geometries that are effectively one-dimensional (Casimir stability considerations).

Disorder in quantum vacuum

Localization of matter waves

- Waves propagating in disordered potentials undergo multiple scattering processes that strongly affect their usual diffusive transport and can result in localized states.

- Recently localization of a 1D BEC has been observed: in a speckle potential (Aspect group, 2008) and in a bi-chromatic optical potential (Inguscio group, 2008)

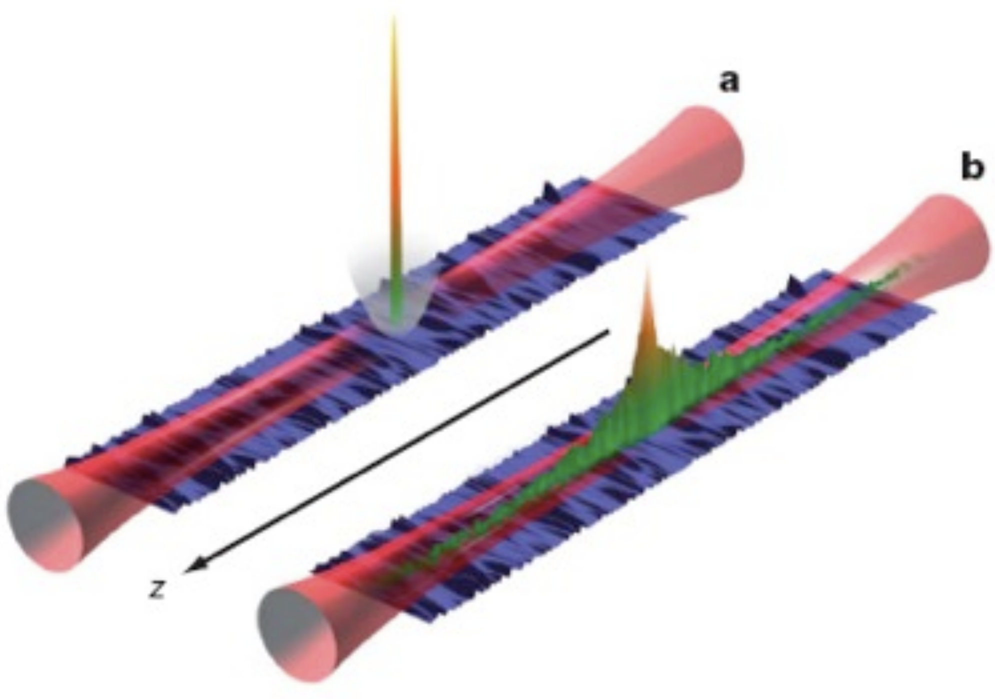

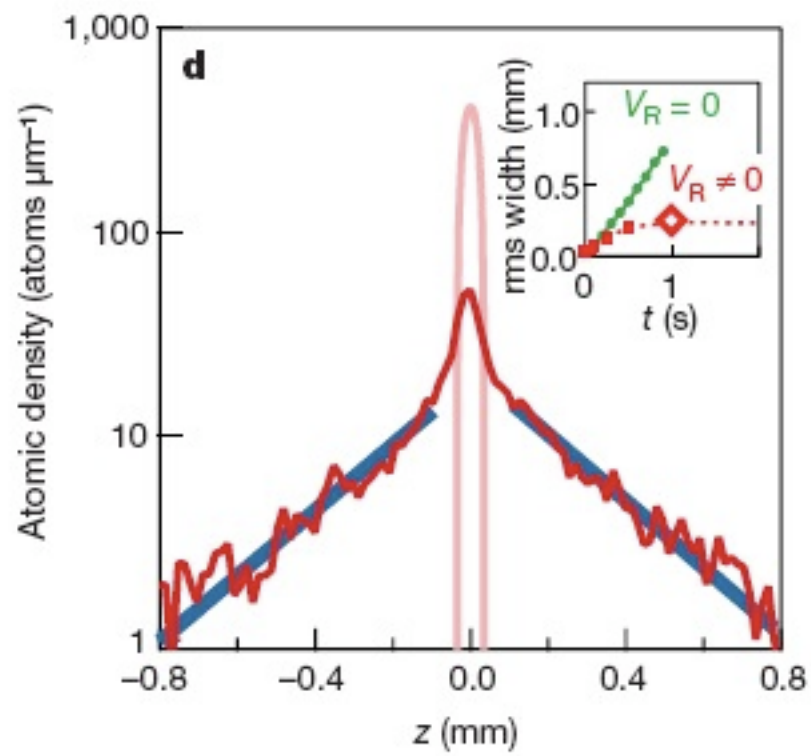

CP for rough surface

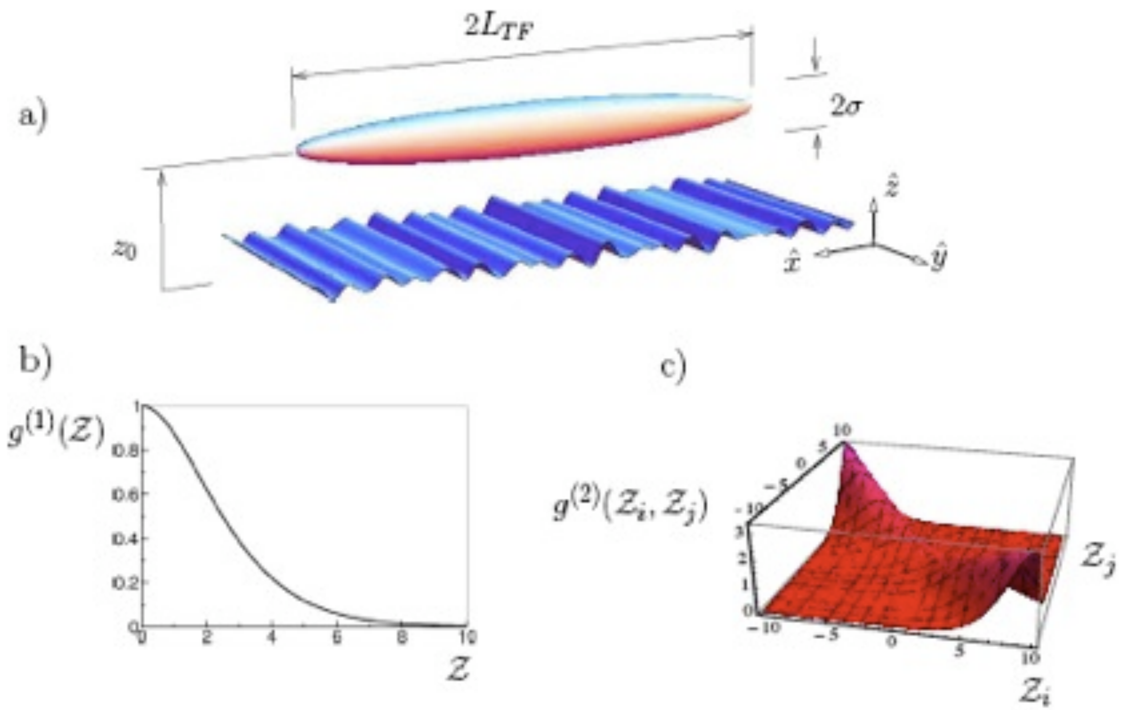

Moreno, Messina, DD, Maia Neto, Reynaud, Lambrecht, PRL 2010

$$h(x) = \sum_{i=1}^{\infty} h_i \cos(k_i x + \theta_i)$$

$$U_L^{(1)}(x,z) = -\frac{3\hbar c\alpha(0)}{8\pi^2\epsilon_0 z^5} \sum_{i=1}^{\infty} h_i\, g^{(1)}(k_i z)\, \cos(k_i x + \theta_i), \quad (1)$$

$$\begin{aligned} U_L^{(2)}(x,z) &= -\frac{15\hbar c\alpha(0)}{32\pi^2\epsilon_0 z^6} \sum_{i,j=1}^{\infty} h_i h_j \qquad (2) \\ &\times \left[\cos((k_i + k_j)x + \theta_i + \theta_j) g^{(2)}(k_i z, k_j z) \right. \\ &\left. + \cos((k_i - k_j)x + \theta_i - \theta_j)\, g^{(2)}(k_i z, -k_j z)\right], \end{aligned}$$

BEC dynamics + weak disorder

Los Alamos NATIONAL LABORATORY

- GP equation

$$i\hbar\,\partial_t\varphi(x,t) = -\frac{\hbar^2}{2m}\partial_x^2\varphi(x,t) + U_L(x,z_0)\Theta(t)\,\varphi(x,t)$$
$$+\frac{m\omega_x^2 x^2}{2}\Theta(-t)\,\varphi(x,t) + g_{\text{eff}}|\varphi(x,t)|^2\varphi(x,t), \quad (3)$$

- Weak disorder: $V_{\mathrm{R}}(z_0) \ll \mu$

$$V_{\mathrm{R}}^2(z_0) = \overline{(U_L(x,z_0) - \overline{U_L(x,z_0)})^2}$$

short-times: interactions dominant, disorder negligible

large-times: disorder dominant, interactions negligible

$$\overline{n(x)} = \frac{3N\xi}{2}\int_0^{1/\xi}(1-k^2\xi^2)\,\overline{|\phi_k(x)|^2}\,\mathrm{d}k\;, \qquad (4)$$

$$\overline{|\phi_k(x)|^2} = \frac{\pi^2\gamma(k)}{2}\int_0^\infty u\sinh(\pi u) \qquad (5)$$
$$\times\left(\frac{1+u^2}{1+\cosh(\pi u)}\right)^2 e^{-2(1+u^2)\gamma(k)|x|}\,\mathrm{d}u.$$

$\xi = \hbar/\sqrt{4m\mu}$ is the healing length of the BEC

CP disorder correlation

$$C(|x - x'|; z_0) = \overline{U_L(x, z_0)\, U_L(x', z_0)}\,.$$

$$\gamma(k) = \frac{m}{4\hbar^2 E_k} \int_{-\infty}^{\infty} C(x) \cos(2kx) dx \qquad E_k = \hbar^2 k^2 / 2m$$

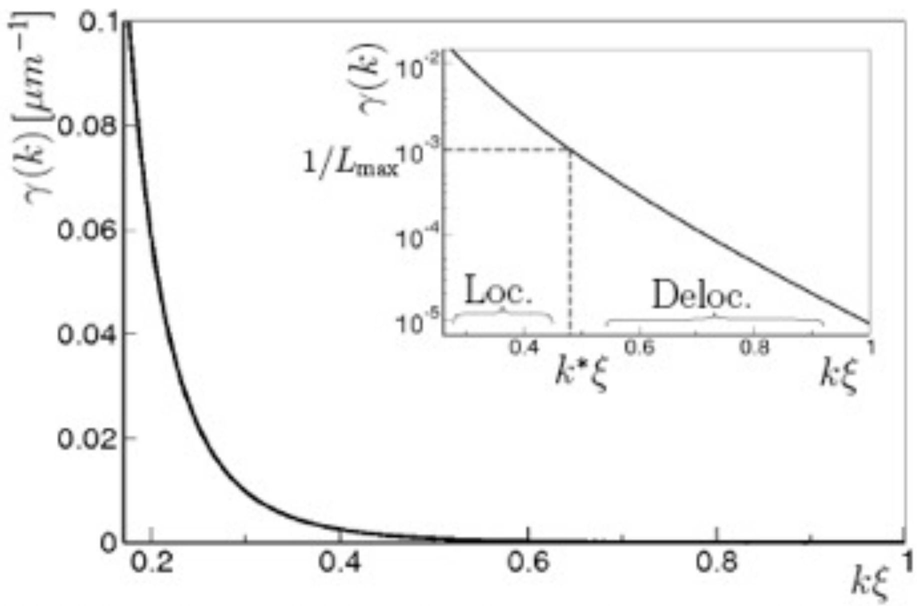

FIG. 2: $\gamma(k)$ vs. $k\xi$ from Eq.(6). The atom-surface distance is $z_0 = 1.5\mu$m. Inset: same data in Log-Lin scale, the maximum length scale to be measured $L_{\max} = 1$mm, and the value $k^* = \gamma^{-1}(1/L_{\max})$ separating localized (Loc.) from delocalized (Deloc.) modes.

$$\gamma(k) = \frac{m\pi^2 F^2(z_0)}{2\hbar^2 E_k (2k)^2}\, \overline{h(x)^2}\, P(\pi/k) \left(g^{(1)}(2kz_0)\right)^2, \quad (6)$$

$$F(z_0) = 3\hbar c\alpha(0)/8\pi^2\epsilon_0 z_0^5.$$

CP-induced localization

$z_0 = 1.5\mu\text{m}$ $\quad V_R = 0.089\,\mu$

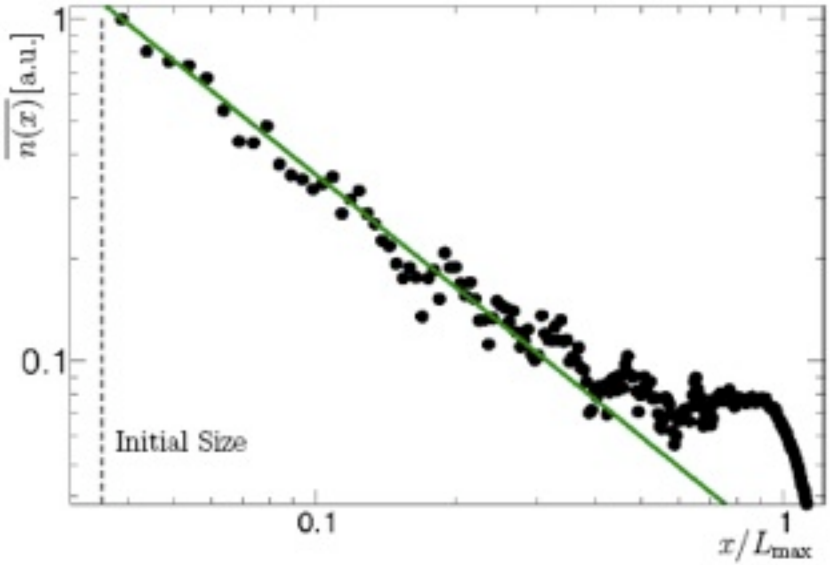

FIG. 3: BEC density (arbitrary units) vs. position. Both the perturbative theory described by Eqs.(4,5,6) (solid) and the full numerical simulation (dots) are computed using the first order approximation for the CP potential at $z_0 = 1.5\mu$m. The surface profile is averaged over 40 realizations. Time corresponds to $\omega_x t = 28$.

$z_0 = 1.0\mu\text{m}$ $\quad V_R = 0.5\mu$

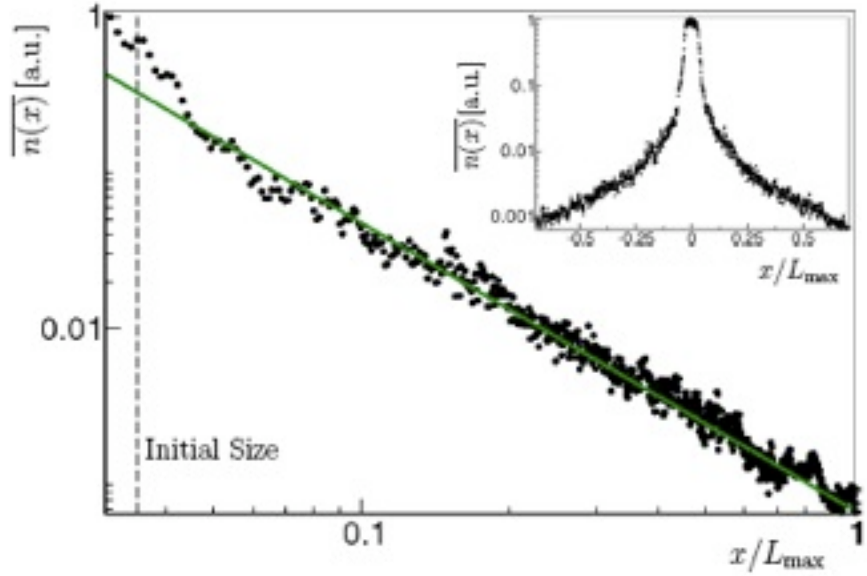

FIG. 4: BEC density (arbitrary units) vs. position, after $\omega_x t = 14$. The profile is averaged over 40 realizations at a distance of $z_0 = 1.0\mu$m. Numerical simulation (dots) includes both the first and second order terms of the lateral CP potential $U_L(x, z)$. The wing is fitted by a power law $\overline{n(x)} \propto 1/x^{\nu}$ with $\nu = 1.84$ (solid). Inset: zoom of the numerical data in Log-Lin scale.

$N = 100\ {}^{87}\text{Rb atoms}$

$\sigma = 0.25\mu\text{m}$ (i.e., radial trapping frequency $\omega_r = 2\pi \times 286\text{Hz}$)

$L_{TF} = 35\mu\text{m}$ (i.e., $\omega_x = 2\pi \times 2.75\text{Hz}$)

$\xi = 0.85\mu\text{m}$.

$h_i \in [0, 200]\text{nm}$

$\theta_i \in [0, 2\pi]$,

$\lambda_i \in [1, 20]\mu\text{m}$

The thermal Casimir force

First observation of the thermal Casimir force

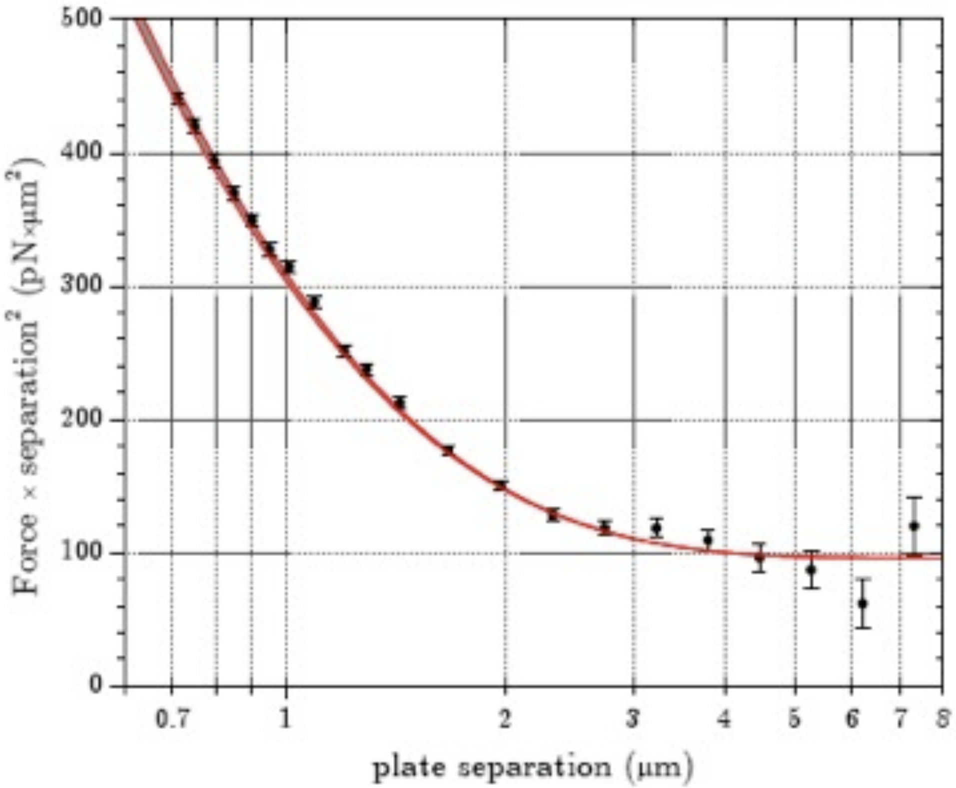

arXiv:1011.5219

Sushkov (Yale), Kim (Seattle), DD (LANL), and Lamoreaux (Yale)

Torsional Pendulum Set-up

✱ Upgrade of Lamoreaux's 1997 experiment

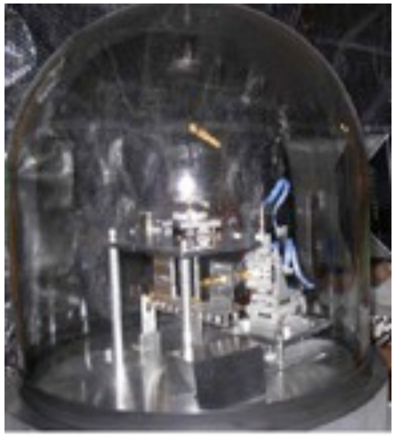

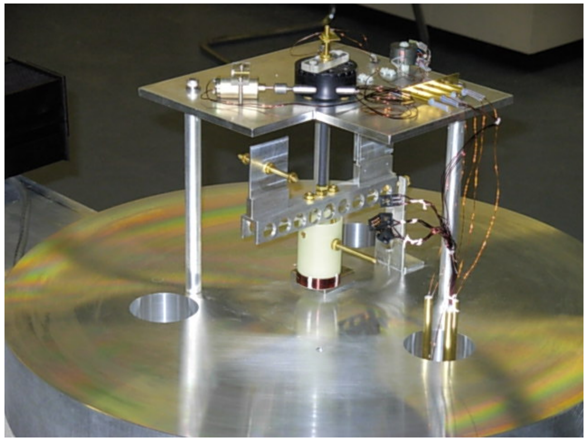

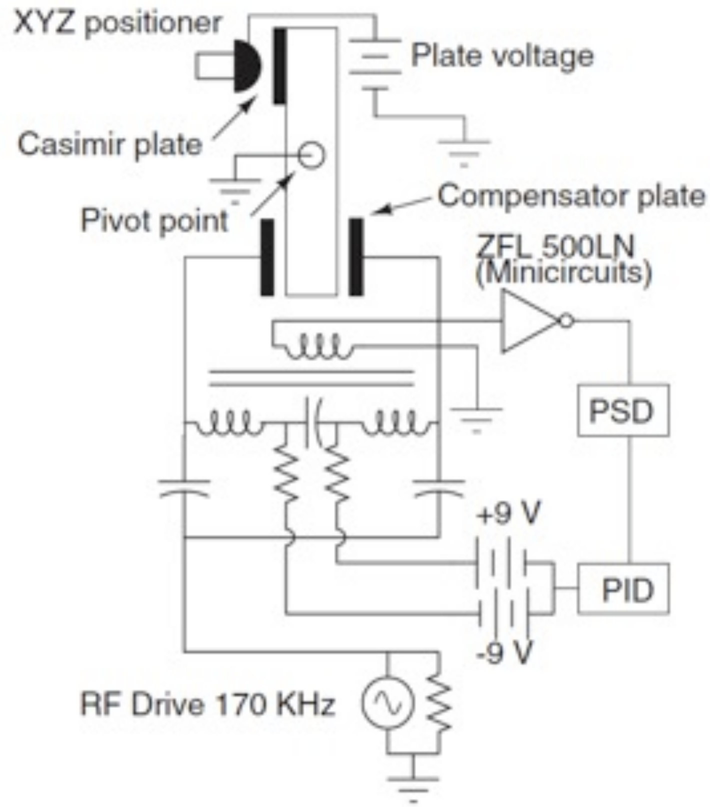

An imbalance in capacitance is amplified and sent to a phase sensitive detector (PSD), which generates error signals.

A proportional integro-differential (PID) controller provides a feedback correction voltage $S_{\rm PID}(d, V_a)$ to the compensator plates, restoring equilibrium.

$$F \propto (S_{\rm PID} + 9V)^2 \approx (9V)^2 + 2S_{\rm PID} \times 9V$$

The correction voltage is the physical observable, and it is proportional to the force between the Casimir plates

Typical Casimir Measurement

$$S_{\mathrm{PID}}(d, V_a) = S_{\mathrm{dc}}(d \to \infty) + S_a(d, V_a) + S_r(d)$$

force-free component of signal at large separations

electrostatic signal in response to an applied external voltage

residual signal due to distance-dependent forces, e.g. Casimir

The electrostatic signal between the spherical lens and the plate, in PFA ($d \ll R$), is

$$S_a(d, V_a) = \pi\epsilon_0 R(V_a - V_m)^2/\beta d$$

β force-voltage conversion factor

This signal is minimized ($S_a = 0$) when $V_a = V_m$, and the electrostatic minimizing potential V_m is then defined to be the contact potential between the plates.

"Parabola" measurements

Calibration routine (Iannuzzi et al, PNAS 04)

A range of plate voltages V_a is applied, and at a given nominal absolute distance the response is fitted to a parabola

$$S_{\mathrm{PID}}(d, V_a) = S_0 + k(V_a - V_m)^2$$

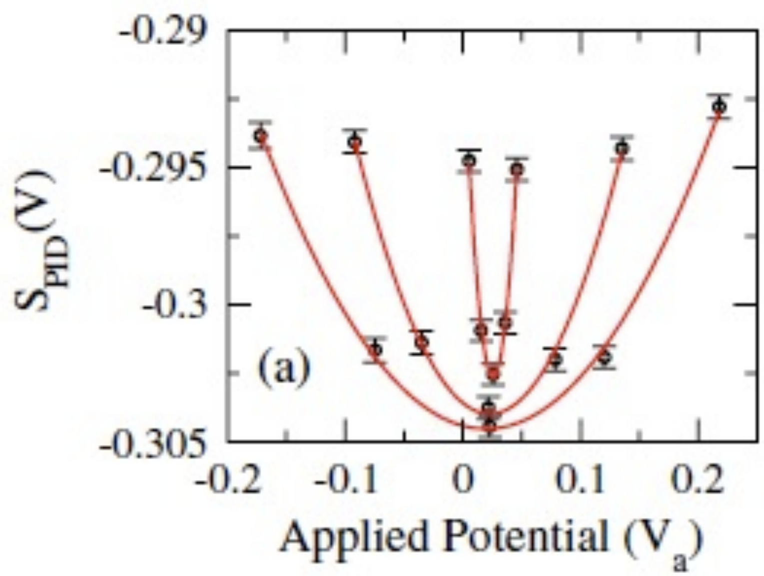

Fitting parameters

$k = k(d)$ ⟶ voltage-force calibration factor + absolute distance

$V_m = V_m(d)$ ⟶ distance-dependent minimizing potential

$S_0 = S_0(d)$ ⟶ force residuals: electrostatic + Casimir + non-Newtonian gravity + ...

This procedure is repeated at decremental distances, from 7 um down to 0.7 um, completing a single experimental run.

In the experiment $V_m = V_m(d)$ is almost constant (0.2 mV variation in the whole range)

Force Residuals

Residuals from Coulomb force obtained from the value of the PID signal at the minima of each parabola,

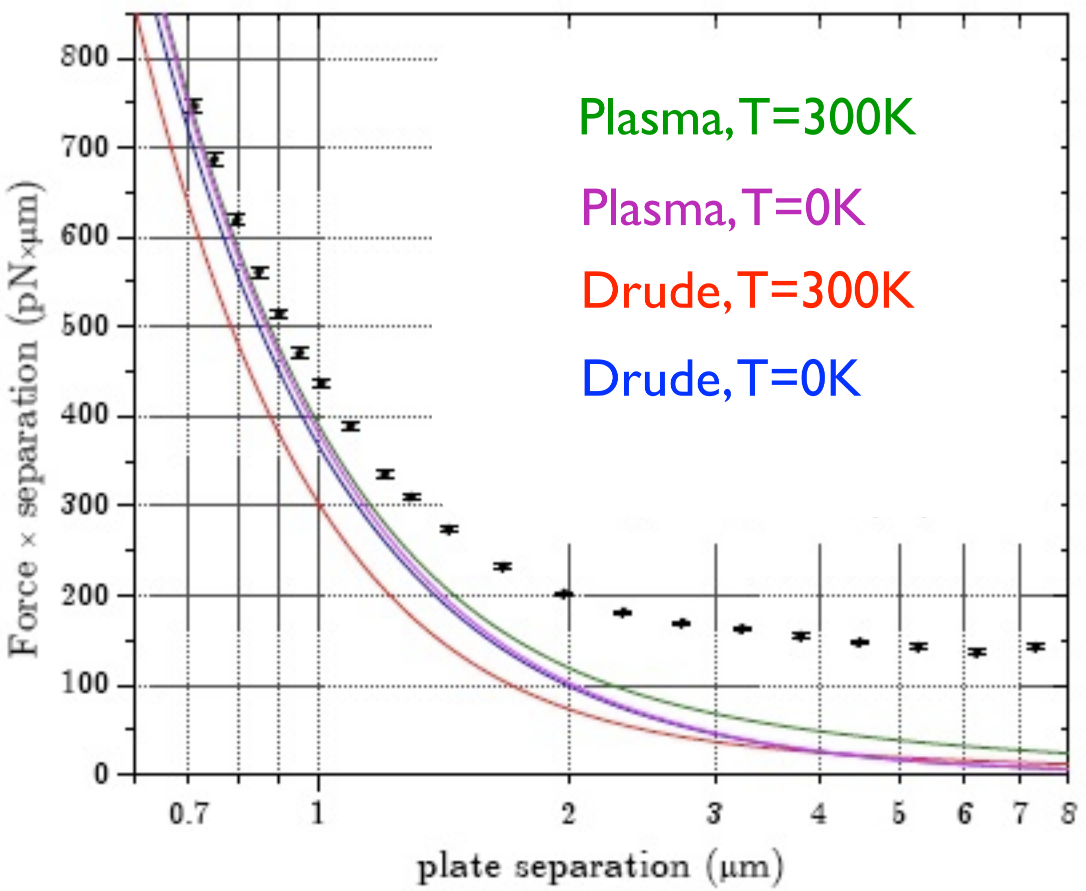

In the experiment, these force residuals are *too large* to be explained just by the Casimir-Lifshitz force between the Au plates.

Electrostatic Patch Effects

Sphere-plane geometry:

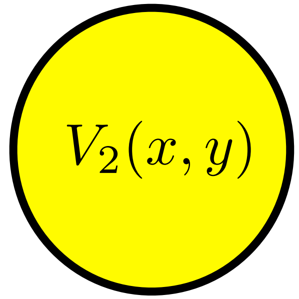

$$\nabla^2 V(x,y,z) = 0$$

$$\boxed{V(z=0) = V_1(x,y)}$$

To compute the patch effect in the sphere-plane configuration we use PFA for the curvature effect $(d \ll R)$ but leave kd arbitrary

$$F_{sp}(d) = 2\pi R \langle U_{pp}(d) \rangle = \frac{\epsilon_0 R}{16} \int_0^\infty dk \, \frac{k^2 e^{-kd}}{\sinh(kd)} \left[C_{1,k} + C_{2,k} \right]$$

Different models to describe surface potential fluctuations:

- $C_{1,k} = C_{2,k} = V_0^2$ for $k_{\min} < k < k_{\max}$

$$F_{sp} = \frac{4\pi\epsilon_0 V_{\rm rms}^2 R}{k_{\max}^2 - k_{\min}^2} \int_{k_{\min}}^{k_{\max}} dk \frac{k^2 e^{-kd}}{\sinh(kd)}$$

- $\mathcal{R}(r) = \begin{cases} V_0^2 & \text{for } r \leq \lambda, \\ 0 & \text{for } r > \lambda. \end{cases}$

$$F_{sp} = 2\pi\epsilon_0 R \int_0^\infty du \, u \frac{J_1(u)}{e^{2ud/\lambda} - 1}$$

In the limit of large patches $(kd \ll 1)$:

$$\boxed{F_{sp}(d) = \pi \epsilon_0 R \frac{V_{\rm rms}^2}{d}}$$

Understanding elec. residuals

We fit the data for the *residual force at the minimizing potential* with a force of equal to Casimir + patch effect

$$\boxed{F_r(d) = F_C(d) + \pi\epsilon_0 R \frac{V_{\rm rms}^2}{d}}$$

Drude, T=300K

Drude, T=0K

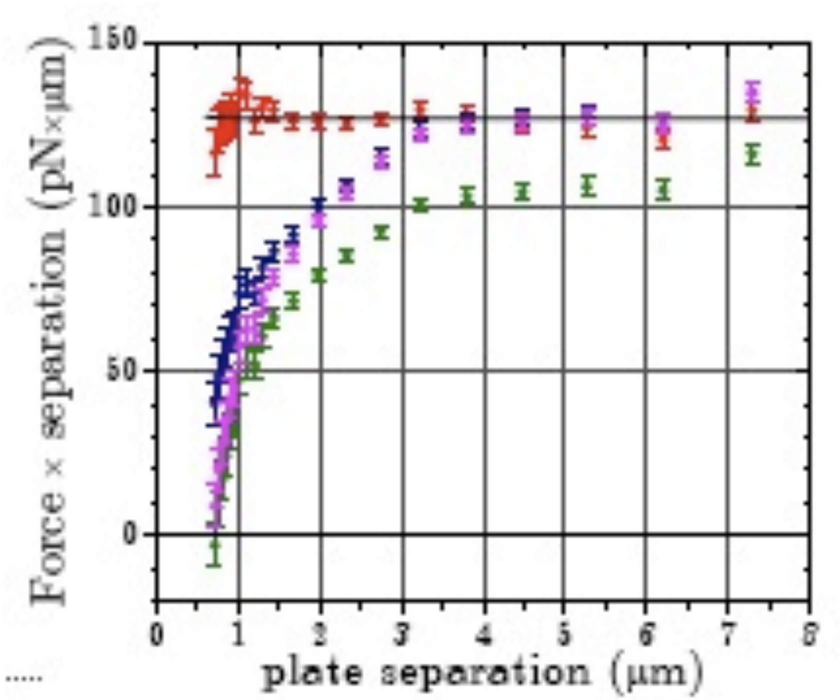

Plasma, T=300K

Plasma, T=0K

Thermal Casimir force

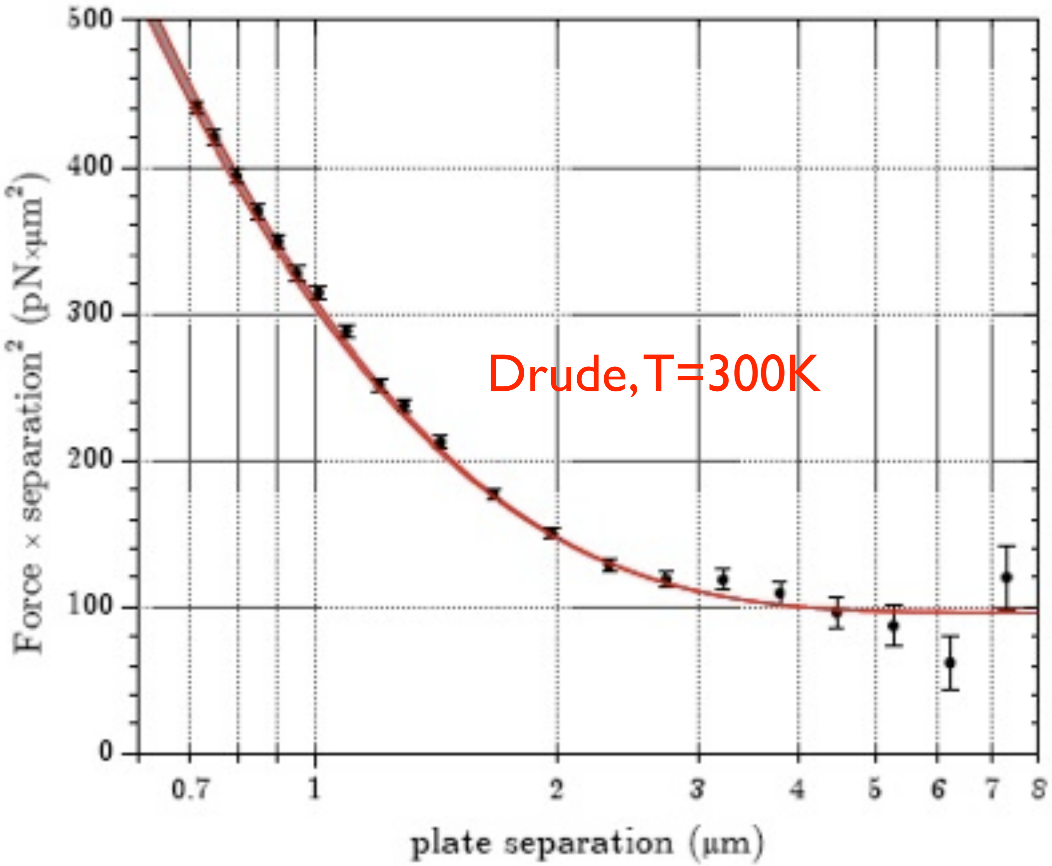

$$F_C^{(T)}(\text{Drude}) = \frac{\xi(3)}{8}\frac{Rk_BT}{d^2}$$

Quality of fits:

	χ^2_{red}	$V_{\text{rms}}(\text{m}V)$
Drude, T=300K	1.04	5.4
Plasma, T=300K	32	3.0
Drude, T=0K	23	4.0
Plasma, T=0K	43	3.6

Remarks:

- Experiment rules out the plasma model in the separation range 0.7um to 7um, and confirms the Drude model

- Thermal correction to the Casimir force demonstrated.

- Electrostatic residuals modeled as due to large electrostatic patches

$$F_r^{\mathrm{patches}} \propto R \frac{V_{\mathrm{rms}}^2}{d} \qquad (\lambda_{\mathrm{P}} \gg d)$$